Performance of European chemistry transport models as function of horizontal resolution

M. Schaap, C. Hendriks, R. Kranenburg

TNO innovation for life

C. Cuvelier, P. Thunis,

European Commission

H. Fagerli, D. Simpson, M. Schulz,

Norwegian Meteorological Institute met.no

A. Colette, E. Terrenoire, B. Bessagnet, L. Rouïl

INERIS

R. Stern

Freie Universität Berlin

A. Graff

Umwelt Bundes Amt
Für Mensch und Umwelt

Main findings

The exercise showed that the model responses to an increase in resolution show a broadly consistent picture among all models.

It should be noted that the response is more significant for CHIMERE simulations compared to the other participating models. It seems to be due to a specific treatment of the mixing parameterization over urban areas. This point is still investigated by INERIS with sensitivity analyses.

The analysis showed that the grid size does not play a major role for air quality model calculations, which are targeted on the determination of the background (non-urban) air quality. Downscaling model resolution does not change concentration estimations and model performance at rural and EMEP sites.

The grid resolution plays an important role in agglomerations characterized by high emission densities. The urban signal, i.e. the concentration difference between high emission areas and their surroundings, usually increases with decreasing grid size. This grid effect is more pronounced for NO2 than for PM10, because a large part of the urban PM10 mass consists of secondary components. This part of the PM10 mass is less affected by a decreasing grid size in contrast to the locally emitted primary components.

The grid effect differs between urban regions. The strength of the urban signal is a function of local emissions conditions (extension of the emission areas, emission density, emission gradient, etc.) and meteorological conditions determining ventilation efficiency. For similar emission conditions, regions with weak wind conditions will show a stronger urban signal than well ventilated regions.

For all models, increasing model resolution improves the model performance at stations near large conglomerations as reflected by lower biases for all components and increased spatial correlation for primary components.

As about 70% of the model response to grid resolution is determined by the difference in emission strength, improved knowledge on spatial variation in emission at high resolution is key for the improvement of modeled urban increments. For this purpose one relies on the replacement of currently used top-down European wide data with national expertise.

It is difficult to define a grid size that is adequate to resolve the urban signal under all conditions occurring in a European-wide modeling area. It has been shown before that, ideally, a grid size in the range of a few km down to 1 km should be chosen. Such a small grid size is not feasible for regional model applications because the data demands and operating requirements are far too large. If the main emphasis of a model application is targeted on the determination of background air quality for rural areas and large agglomerations, the grid scale M2 (28 Km) or, if the data and operational requirements can be fulfilled, the grid scale M3 (14 Km) seems to be a good compromise between a pure background application and an application which reproduces most of the urban signals (M4 resolution or even higher).

The limited impact on regional scale model performance shows that a continuing effort is needed to better understand atmospheric processes and interactions with the surface, and to improve our knowledge on emissions (amount, speciation, location and timing).

Table of contents

1. Introduction

The EMEP models (www.emep.int) have been instrumental to the development of air quality policies in Europe since the late 1970s. In the 1990s the EMEP models became also the reference tools for atmospheric dispersion calculations as input to the Integrated Assessment Modelling, which supports the development of air quality polices in the European Union. Since 1999, the EMEP model has been run on a resolution of 50 * 50 km^2 resolution. However, the last years, modification of the EMEP grid has been discussed, an important aspect of which is the grid resolution. An increase in model resolution requires that the input data (most importantly the emissions) are available on the same scale. As an increase in model resolution will increase the computational costs cubically, it is important to determine the "optimum resolution", at which scale the improvement in resolution does not give improvement in performance any longer and for which the computational effort is not too large.

To support EMEP in this decision, an initiative was taken for a model inter-comparison exercise aimed at analysing the model performance of the different chemical transport models as a function of model resolution. Six modelling teams participate in the exercise: EMEP, LOTOS-EUROS, CHIMERE, RCG, CAMx and DEHM. All models were to perform four runs for Europe on different resolution. The specifics of the models and the experimental set-up are described in section 2. A (statistical) evaluation of the performance of the models on different resolutions is presented in section 3. Note that the study is still ongoing. In this document results from four models are presented. The full dataset will be completed in fall, after which a more detailed analysis of the model responses is foreseen. Therefore, section 4 presents the most important findings from this exercise so far as input to the 2012 EMEP Steering Board meeting.

2. Methodology

2.1 Simulations

By each modeling team four model simulations were carried out with different horizontal resolutions. The simulations were performed for the year 2009 for the EC4MACS domain encompassing Europe (Figure 1). Four resolutions were used doubling the resolution between each simulation. Four resolutions were used doubling the resolution between each simulation. The spatial resolution ranges from a 1.0x0.5 degrees (56x56 km) resolution to 0.125 x 0.0625 degrees (7x7 km) resolution. As the high resolution simulation is very demanding in terms of computing power the EC4MACS domain encompasses southern and central Europe completely, but cuts of the remote area in northern Scandinavia.

The anthropogenic emission input was harmonized by using a common EC4MACS emission dataset. The emission dataset was delivered by INERIS for all model resolutions separately. Except for SNAP 2, prescribed time profiles and height distributions were used following the EURODELTA protocol (REF). For SNAP2 daily gridded modulation factors were calculated based on temperature days (REF). For the SNAP 2 hourly variation the EURODELTA hour-of-the-day profile was used.

All other input parameters were not prescribed. This means that the models use different meteorological input data as well as land use data. In case of meteorology most models use data from ECMWF, whereas RCG used diagnostic meteorology from TRAMPER. Boundary conditions derive from global model climatological data or simulations as well as experimental derived climatological data. For a more detailed specification of the model and its input data we refer to Table 1-2.

Table 1 : Domains definition

Domain	**nx**	**ny**	**Lon. Res.**	**Lat. Res.**	**Kilometre scale**	**SW starting point Lon/Lat (grid centres)**
EC4M1	41	52	1.0	0.5	56x56	-10.000 / 36.125
EC4M2	82	104	0.5	0.25	28x28	-10.250 / 36.000
EC4M3	164	208	0.25	0.125	14x14	-10.3750 / 35.9375
EC4M4	328	416	0.125	0.0625	7x7	-10.43750 / 35.90625

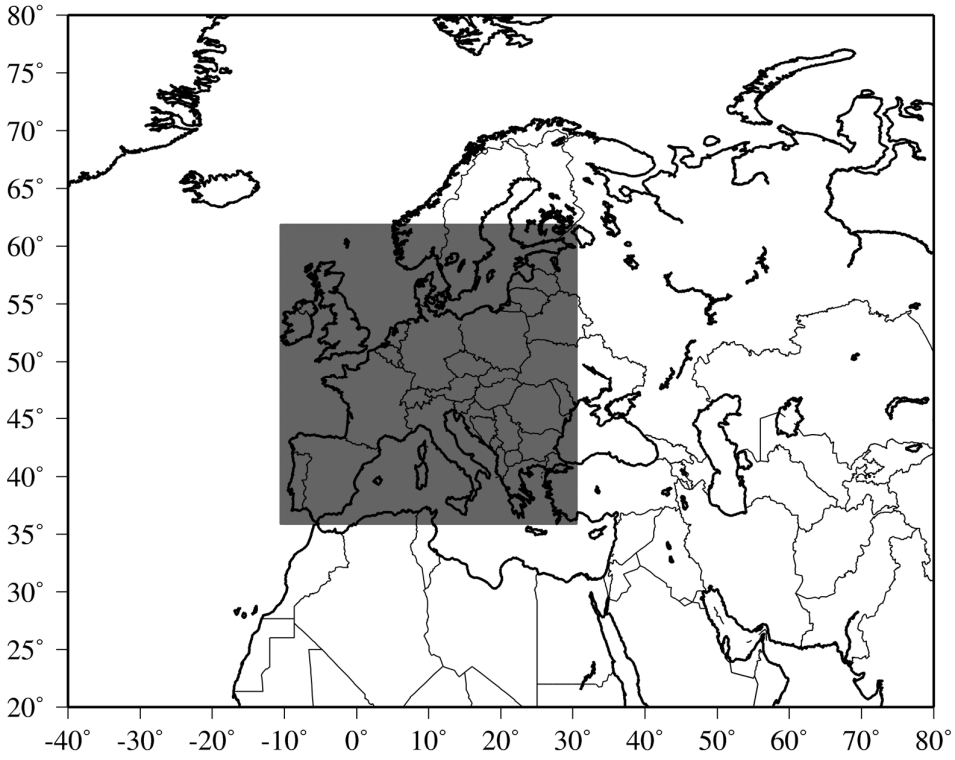

Figure 1 : Domain broken down in 4 resolutions types

The output required for the exercise was prescribed and contains hourly as well as daily concentration distributions across Europe (Table 2). The output species contain the oxidants as well as particulate matter, its components and precursor species. Besides concentrations also deposition fields were requested to be able to perform a first order assessment of the representation of atmospheric input to eco-systems.

Table 2. Proposed model output parameters

Time resolution	PM & components	Gases	Deposition Fluxes	Meteorology
Hourly	PM2.5, PM10	O3, NO2, NO	-	U10, T2m, Kz, PBL, u*
Daily	PM2.5, PM10 PPM_fine, PPM_coarse NO3_f, NO3_c SO4_f, SO4_c NH4_f, NH4_c SOA_f, SOA_c Dust_f, Dust_c SS_f, SS_c	SO2, NH3, HNO3	D_NOx, D_SOx, D_NHx, W_NOx, W_SOx, W_NHx	Rain amount

2.2 Participating chemistry transport models

In this study six eulerian CTMs are applied to address the sensitivity of the model performance for ozone, particulate matter and nitrogen dioxide. The participating model systems are:

- EMEP
- LOTOS-EUROS
- CHIMERE
- RCG
- CAMx
- DEHM

In tables 1-2 the main characteristics of these model systems are listed. For detailed model descriptions we refer to the literature on these models. In the appendices, we introduce the models shortly.

All models have kept there model codes the same for each resolution. The expected change in concentrations due to an increase in resolution is therefore due to the much sharper gradients in the emissions and the sensitivities of process descriptions to concentration differences. Also, the land use data are available as a mosaic at high resolution, meaning that the 7 Km cells inside a 56 Km cell will have the same land cover total per land use class but that they are also allocated with more detail at the higher resolution. All models interpolate the input meteorological data to the required model resolution.

On exception should be mentioned. Within CHIMERE an adjustment is made to mixing parameters above urban areas. This means that this adjustment is different in the simulations performed here with many more model grid cell defined urban at 7 Km resolution than at the coarser resolutions. The full motivation by the CHIMERE team is given in the appendix (6.2). Instead of applying a correcting profile to downscale the model outputs near the ground, the CHIMERE pre-processing was modified to diagnose an improved urban meteorology. In short, they argue that the mixing in the urban environment within the canopy layer is overestimated with standard similarity theory. Therefore, the Kz in the first CHIMERE layer above urban areas is modified as follows:

$$Kz\ (z < first\ level) = \frac{Kz\ (first\ level\ computed\ with\ the\ similarity\ theroy)}{2}$$

This coefficient (factor 2) is also applied to lower the wind speeds in the first CHIMERE layer so as to limit the advection and dilution of primary pollutants close to the ground.

Table 3. Overview of model characteristics

Model	EMEP	LOTOS-EUROS	CHIMERE	RCG
version number	rv4beta12	v1.8		v2.1
operator	met.no	TNO/KNMI/RIVM	INERIS/IPSL-CNRS	FU Berlin
contact	David Simpson	Martijn Schaap	Bertrand Bessagnet	Rainer Stern
email	david.simpson@met.no	martijn.schaap@tno.nl	bertrand.bessagnet@ineris.fr	rstern@zedat-fu-berlin.de
Vertical model structure				
vertical layers	20 sigma	4 (3 dynamic layers and a surface layer)	9 sigma	4 sigma
Vertical extent	100 hPa	3500 m	500 Hpa	3000 m
Depth first layer	90 m	25 m	20 m	25 m
NATURAL EMISSIONS				
BVOC	Based upon maps of 115 species from Koeble and Seufert, and hourly temperature and light. See Simpson et al., 2012	Based upon maps of 115 species from Koeble and Seufert, and hourly temperature and light. See Schaap et al., 2009	MEGAN model	Based upon maps of 115 species from Koeble and Seufert, and hourly temperature and light.using emissions factors of Simpson et al. (1999).
forest fires	FINNv1, daily	MACC forest fires	Monthyl GFED3 database	none
Soil-NO	Simpson et al. (2012)	Not used here	MEGAN model	Simpson et al. (1999)
Lightning	Climatological fields, Köhler et al. (1995)	none	none	none
Sea salt	Tsyro et al. (2012)	Martensson et al., 2006 and Monahan et al., 1986	Monahan et al., 2006	Gong et al. (1997) and Monahan et al. (1986)
Windblown Dust	Simpson et al., 2012	Schaap et al. (2009) Not used here	Vautard et al. (2005), not used here	Loosemore & Hunt (2000), Claiborn et al. (1998)
Agricultural land management. Dust	None	Schaap et al. (2009), Not used here	none	none
Dust traffic suspension	Schaap et al. (2009)	Schaap et al. (2009), Not used here	none	none
Saharan dust inflow	Not used here	Not used here	Yes	Not used here
LAND USE				
Landuse database	CCE/SEI for Europe, elsewhere GLC2000	Corine Land Cover 2000 (13 classes)	GLOBCOVER (24 classes)	Corine Land Cover 2000 (13 classes)
resolution	Flexible, CCE/SEI ~ 5 km	1/60 x 1/60 degrees	300 m	1/60 x 1/60 degrees
BOUNDARY CONDITIONS				
Ozone and oxidants	As available (from global model or specified)	MOZART 3-hourly	LMDzINCA monthly clim.	O3 monthly clim (Logan, 1998); all other species clim. background values
PM comp.	clim. background values	MOZART 3-hourly	GOCART monthly clim.	clim. background values

Table 4. Overview of model characteristics continued

Model	EMEP	LOTOS-EUROS	CHIMERE	RCG
METEOROLOGY				
description	ECMWF	ECMWF	ECMWF IFS + urban mixing	TRAMPER diagnostic
resolution	0.22 deg x 0.22 deg	1/2 x 1/4 degrees	1/2 x 1/4 degrees	1/2 x 1/4 degrees
PROCESSES				
Advection	Bott (1989a,b)	Walcek (2000)	Van Leer	Walcec (2000) modified by Yamartino (2003).
Vertical diffusion	Kz approach	Kz approach	Kz approach following Troen and Mart, 1986	Kz-approach
Dry deposition	resistance approach, Simpson et al, 2012	DEPAC3.11 / Van Zanten et al.(2010)	resistance approach Emberson (2000a,b)	resistance approach, DEPAC-module
landuse class	16 classes	9 classes	9 classes	9 classes
compensation points	No, but zero NH3 deposition over growing crops	only for NH3 (for stomatal, external leaf surface and soil (= 0))	no	no
stomatal resistance	DO3SE-EMEP: Emberson et al, 2000, Tuovinen et al., 2004. Simpson et al., 2012	Emberson (2000a,b)	Emberson (2000a,b)	Wesely (1989)
wet depsotion gases	In-cloud and sub-cloud scavenging coefficients	pH dependent scavenging coefficients (Banzhaf et al., 2011)	In-cloud and sub-cloud scavenging coefficients	pH dependent scavenging coefficients
Wet deposition particles	In-cloud and sub-cloud scavenging	In-cloud and sub-cloud scavenging	In-cloud and sub-cloud scavenging	In-cloud and sub-cloud scavenging
Gas phase chemistry	EmChem09	TNO-CBM-IV	MELCHIOR	CBM-IV
Cloud chemistry	Aqueous SO2 chemistry	Banzhaf et al. (2011)	Aqueous SO2 chemistry	Aqueous SO2 chemistry
Coarse nitrate	yes	yes	no	no
Ammonium nitrate equilibrium	MARS	ISORROPIA2	ISORROPIA (Nenes et al., 1998)	ISORROPIA
SOA formation	VBS-NPAS –Simpson et al. (2012)	not used	After Bessagnet et al., 2009	SORGAM module (Schell et al., 2001)
VBS	Yes, Bergström et al (2012), Simpson et al. (2012)	not used	no	none
Aerosol model	Bulk- approach (2 modes)	Bulk- approach (2 modes)	8 bins (40 nm - 10 µm)	Bulk- approach (2 modes)
Aerosol physics	not used	not used	coagulation/condensation/nucleation	none

2.3 Definition of PM10

The participating models differ in the availability of PM components and formation routes. For instance, EMEP and LOTOS-EUROS contain coarse mode nitrate formation, whereas the others do not. Also, CHIIMERE, EMEP and RCG report secondary organic aerosol, where the modeling team from LOTOS-EUROS considers their model formulations too uncertain for use in policy support. The PM10 total concentration is calculated as follows in the models:

EMEP $PM10 = PPM_{coarse} + PPM_{fine} + SO_4^{2-} + NO_3^- + NH_4^+ + \text{Sea Salt} + SOA + \text{Dust}$

CHIMERE $PM10 = PPM_{coarse} + PPM_{fine} + SO_4^{2-} + NO_3^- + NH_4^+ + \text{Sea Salt} + SOA + \text{Dust}$

LOTOS-EUROS $PM10 = PPM_{coarse} + PPM_{fine} + SO_4^{2-} + NO_3^- + NH_4^+ + \text{Sea Salt}$

RCG $PM10 = PPM_{coarse} + PPM_{fine} + SO_4^{2-} + NO_3^- + NH_4^+ + \text{Sea Salt} + SOA + \text{Dust}$

Hence, the modeled components and therefore the explained mass will differ between models hampering the comparability. Also, the components that are not common (dust, SOA, coarse nitrate) are associated with the largest uncertainties, which may deteriorate certain statistical parameters when included. Hence, we also defined a common PM10 measure that includes the components that all models have:

$PM10\_common = PPM_{coarse} + PPM_{fine} + EC + POM + SO_4^{2-} + NO_3^- + NH_4^+ + \text{Sea Salt}$

This quantity allows for a fair comparison between the different models. Note, that due to the neglection of several components an underestimation is expected as observed in many model evaluation studies and previous model intercomparisons (e.g. Stern et al., 2008; Vautard et al., 2009; Solazzo et al., 2012). However, in this analysis the PM10_common concentrations were not used, so that the PM10 concentrations in the models reflect different compositions.

Table 5. Overview of modelled components that is included in the PM10 and PM2.5 concentration of each model

	Fine mode								Coarse mode				
	SO4	NO3	NH4	PPM	aSOA	bSOA	SS	Dust	SO4	NO3	PPM	SS	Dust
EMEP													
CHIMERE								x					x
LOTOS-EUROS					x	x		x					x
RCG													
CAMx													
DEHM													

Filled = Included in model simulations and reported; x = included in model but not used

2.4 Model evaluation procedure

The impact of the increase of the model resolution on its performance needs to be quantified. As an important feature of the increased resolution should be to better describe horizontal gradients and better resolve the gradients between source regions and the regional background the quantification of the spatial correlations for all resolution is the first analysis performed here. The higher resolution of the emissions and the model may separate rural background monitoring sites from those of urban locations and source areas by the fact that they appear in different model grids. To analyse the improvement in the spatial gradients the spatial correlation, the slope of the best fit and the bias are used. Not only the gradients should be described better, also a small improvement of the temporal representation of the measured times series is expected for primary components. The reason is that plumes of a source regions may or may not hit the station in the high resolution, whereas in the coarse resolution the site could be in the same grid cell and it will always be affected. Hence, the second part of the evaluation focusses on the temporal behaviour looking at correlation coefficients and RMSE. The model to measurement comparison was performed at a central location (JRC) to ensure a harmonised evaluation procedure. For this purpose the DeltaTool (Thunis et al., 2011) developed in the frame of the FAIRMODE activity has been used.

EMEP	AIRBASE
O3	O3
O3_8HrMAx	O3_8HrMAx
NO2	NO2
SO2	PM2.5
NH3	PM10
SO4	
NO3	
NH4	
TNO3	
TNH4	
PM10	

In this exercise monitoring data from two networks were used. The first network is the EMEP network. This network was designed to evaluate regional scale models aimed at correctly describing trans-boundary air pollution. As these models used to have resolutions of 50 – 150 Km when the network was designed, the locations of most stations are at a considerable distance from source areas in rural or remote regions. The only exception is ammonia, as the major ammonia sources are associated with agricultural rural areas. Hence, the EMEP network may not be the most suitable network to investigate the impact of high resolution modelling. Therefore, we also use the AIRBASE database which contains a host of stations located in rural and urban areas. To focus on the representation of gradients around large agglomerations a specific selection of stations was performed as presented below. Note that the AIRBASE network contains only the major pollutants. Hence, particulate matter speciation is addressed using the EMEP network.

2.4.1 EMEP data

The EMEP network is not used to its full extend here. The analysis aimed the urban agglomerations was prioritised as the first evaluation showed little impact of model resolution at rural monitoring stations. See below.

2.4.2 AIRBASE data analysis

To highlight the differences between the model results obtained with the 4 spatial resolutions, we focus the analysis on 30 EU urban areas (Figure 2). Within a radius of 30 km around each city (regardless of the city size) all AIRBASE urban background and traffic stations measurements are used to evaluate the model results and assess the impact of increased resolution. This 30 km radius is chosen because it leads to a surface around each station approximately equal to the area of a 50x50 km EMEP grid cell. The number of stations available within each city area differs from city to city as does the split in terms of station types (rural, urban, traffic). An overview of the stations used per city for the evaluation is provided in Table 1.

Within a radius of 30 km around each city not many rural stations are included in the analysis due to the proximity of the city (as seen from Table 1) To provide some classical evaluation in terms of comparison with rural background stations a larger radius of 200 km has been considered in which all AIRBASE-Rural and EMEP measurement stations have been used and compared to model results.

Although traffic stations are not expected to be adequate to assess performances of models running at these resolutions (7 km or larger) those stations are used in some parts of the analysis to illustrate the difference (between urban background and traffic) in terms of observed values but also to point out the remaining modeling gaps.

It is important to remember that the number of stations included in each of the station groups is different . While the total number of rural stations (R) used to produce the average for PM10 is 13 it reaches 97 for urban stations (Table 6). The weight of the various cities into this average is also a key element which needs to be remembered for the interpretation. While for Warsaw 10 urban background stations are considered, other cities like Stockholm only have one.

This analysis is performed for hourly NO2, daily averaged and daily maximum 8h O3 averages and daily averaged PM10 concentrations and mostly focuses on urban background station types since the increased resolution is expected to have its maximum gain at those stations.

In order to better highlight model differences in terms of urban areas and station types, groups of stations are generated in which statistical performance indicators are averaged.

Finally it is important to note that differences between resolutions should be seen as grid resolution increments rather than urban increments. Indeed in the case of a very large city area characterized by an homogeneous distribution of the emissions, no difference between resolutions should be expected.

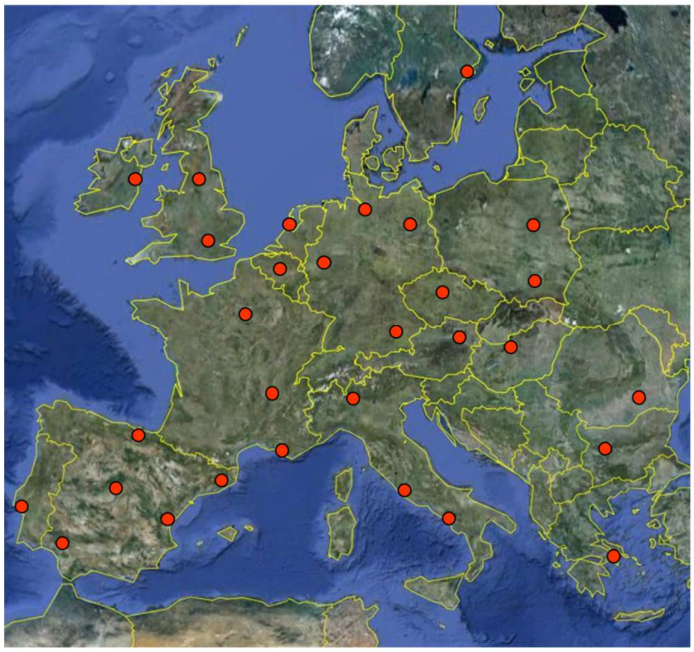

Figure 2. Urban areas selected for the analysis. Available measurements within a radius of 30 km around each city area are selected for urban background and traffic stations. For comparison with AIRBASE rural background and EMEP stations, the selected radius around each stations is 200 km.

Table 6. Overview of the available measurement stations per city, pollutants and station type. For AIRBASE traffic and urban groups a radius of 30 km around each city is assumed whereas for the AIRBASE rural background and EMEP groups, the radius is 200 km.

		PM10				NO2				O3			
		Traffic	Urban	Rural	EMEP	Traffic	Urban	Rural	EMEP	Traffic	Urban	Rural	EMEP
Amsterdam	**AMS**	3	2			8	7	2		2	1	2	
Athens	**ATH**	3		2		6	2			4	2		
Barcelona	**BAR**	14	5			10	5			8	4		
Berlin	**BER**	9	5	3	1	9	6	4			3	4	
Bilbao	**BIL**	1	4	1	1	3	4	1	1	2	4	1	1
Bruxelles	**BRU**	2				4	1	1		2	1	1	
Bucarest	**BUC**	1	1			2		1			1	1	
Budapest	**BUD**	2	1		2	2	1				1		2
Cologne	**COL**	2				2							
Dublin	**DUB**	1	2			2	2				1		
Hambourg	**HAM**	4	6	1	1	5	6	1			2	1	
Krakow	**KRA**		5			1	3				2		
Leeds	**LEE**	1	1			1	2		2		2		3
Lisbon	**LIS**	5	8			5	11			3	10		
London	**LON**	4	3		1	5	5		3	1	5		3
Lyon	**LYO**	1	2	1		2	3	1			3	2	
Madrid	**MAD**	8	5		3	22	7		3	22	7		3
Marseille	**MAR**	2	4	1		2	4	1			1	2	
Milan	**MIL**	5	8	2		9	9	4		1	9	4	
Munich	**MUN**	4	1			5	1			2	1		
Naples	**NAP**	7				7				6			
Paris	**PAR**	2	7			4	19				12		
Prague	**PRA**	8	4		1	8	4			3	2		1
Rome	**ROM**	6	6		1	6	6	1			6	1	
Sevilla	**SEV**	1	2			2	5			1	4		
Sofia	**SOF**	1		1		1		1				1	
Stockholm	**STO**	4	1		1	3	1				1		1
Valencia	**VAL**	5	2		1	8	2		1	6	2		1
Vienna	**VIE**	8	2	1	1	9	4	4			3	3	
Warsaw	**WAR**	1	10			1	6				3		1
Total		**115**	**97**	**13**	**14**	**154**	**126**	**22**	**10**	**63**	**93**	**23**	**16**

3. Results

3.1 Modelled distributions

Figure 3 to Figure 5 how the annual mean concentrations of NO2, O3 and PM10 as calculated for the four different horizontal grid resolutions. For each component another model is used as an example. Figure 3 shows that for NO2 going from the coarse grid M1 to the fine grid M4 the concentration pattern increasingly reflects the underlying emission pattern. The calculated concentrations increase in particular in the high emission density areas. Overall, the increase in structure is tremendous. Especially going from 56 to 14 Km add a lot of detail, whereas the step to 7 Km does not show such a large change in the structure.

Also for PM10 the concentration pattern reflects increasingly the underlying emission pattern going to higher resolution, but much less pronounced than in the case of the NO2 concentrations, because the secondary aerosols, which provide a large part of the total PM10 mass, are much less affected by the grid size than the primary PM components. The calculated concentrations increase in particular in the high emission density areas.

Compared to NO_2 and PM_{10}, the effect of a decreasing grid size is small for ozone. In general, there are only small changes in rural areas. In urban areas, a decrease of the grid size leads also to a decrease of the calculated ozone concentrations as titration by local NO sources is enhanced.

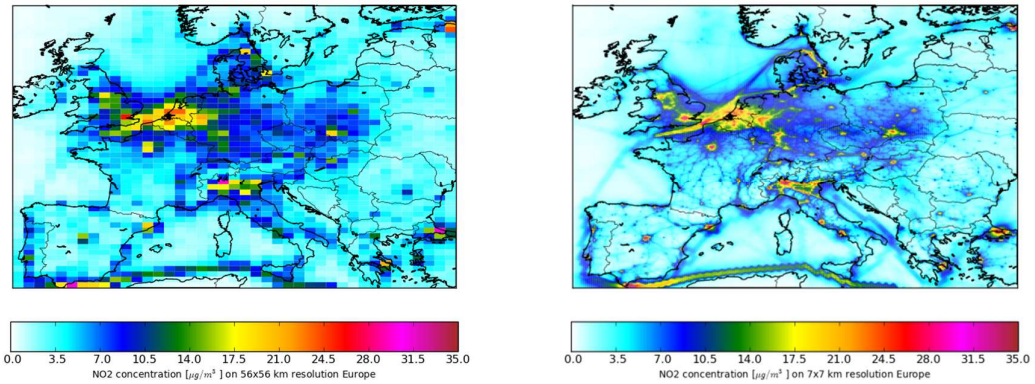

Figure 3. Modelled NO2 distribution (µg/m3) by LOTOS-EUROS for horizontal resolutions of 56 and 7 Km

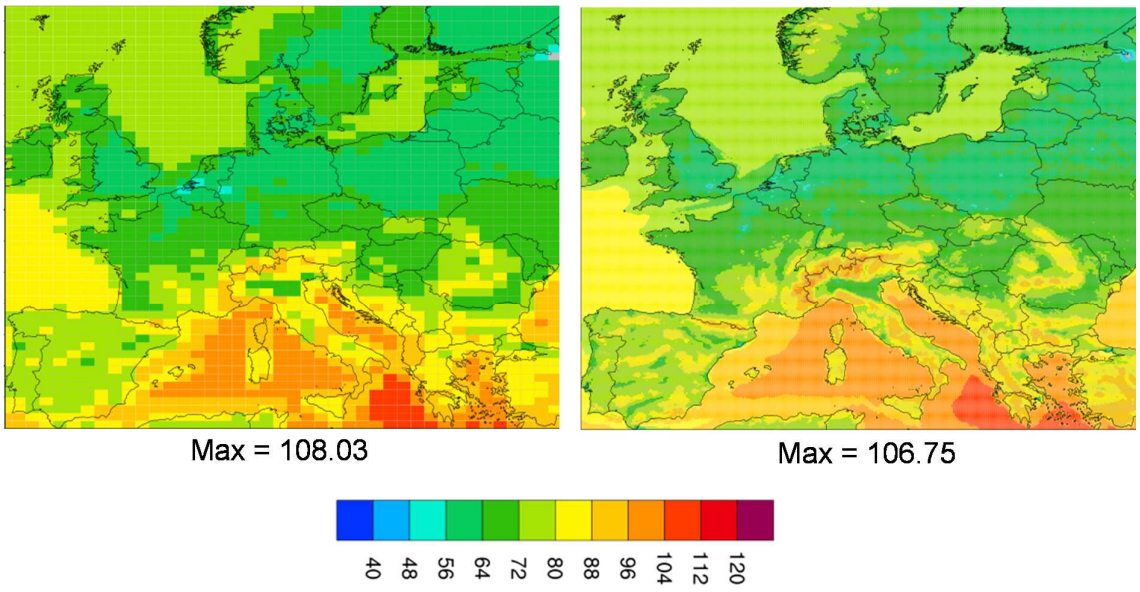

Figure 4. Modelled annual average O3 (ug/m3) by EMEP distributions at 56 and 7 Km

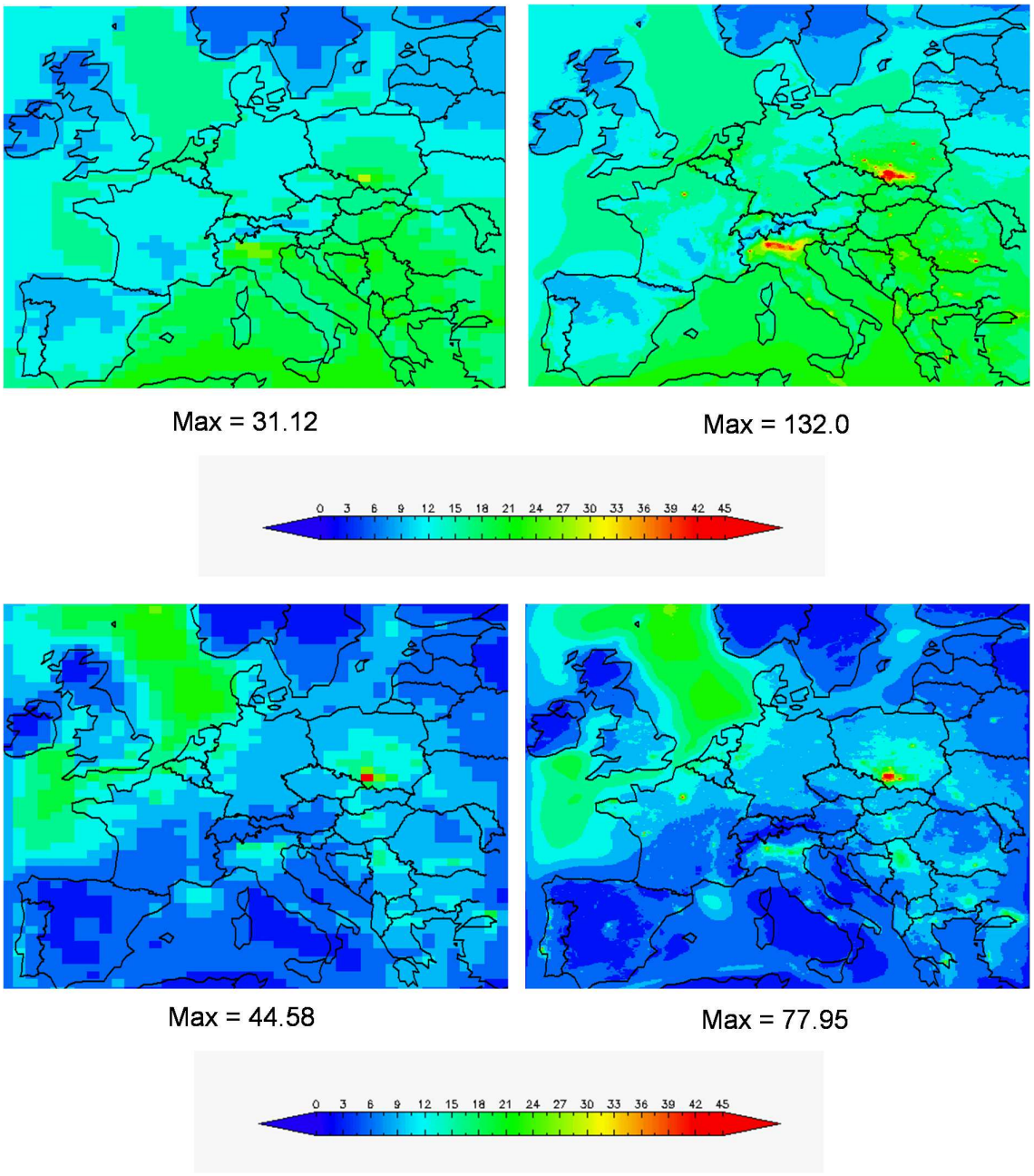

Figure 5. Modelled distributions at 56 and 7 Km for PM10 by CHIIMERE (upper panels) and RCG (lower panels)

3.2 Scale dependency of model performances in terms of speciation for the EMEP network

The evaluation of the model performance at the EMEP network stations has not been performed at the central JRC site so far. The reason is that the data on the PM speciation were not available yet for all models and, more importantly, the measurement data were not yet prepared for use in the DELTA tool at this stage of the exercise.

First analyses for the EMEP and LOTOS-EUROS models show that the model performance at the EMEP stations is hardly affected by the change in resolution. Thereby they confirm the picture for the rural stations presented below.

EMEP stations are however used for analyzing the scale dependency performances on PM total mass, NO2 and O3

3.3 Scale dependency of model performances for the AIRBASE analysis

3.3.1 NO2

As seen in Figure 6 where the annual average NO2 concentrations are grouped by station types (i.e. all station belonging to a station type are grouped together), the grid resolution increment is as expected very weak at rural and EMEP stations. It is interesting to note the small decrease of NO2 modelled at the EMEP stations. All models agree with a negligible impact at rural and EMEP stations and on the trends at traffic and urban stations. Although the magnitude differs between models, the gain resulting from an increased resolution is significant for urban stations (more than 10 µg/m3) and traffic stations (same order of magnitude). Largest increments seen for CHIMERE and RCG and slightly lower responses for the other models. Largest gains seem to be between 56 and 28 and from 28 to 14 Km (EMEP, LOTOS-EUROS), though RCG yields similar increases for each step in resolution. CHIMERE reacts stronger to the resolution change than the others due to the adjustment of mixing parameters in urban areas.

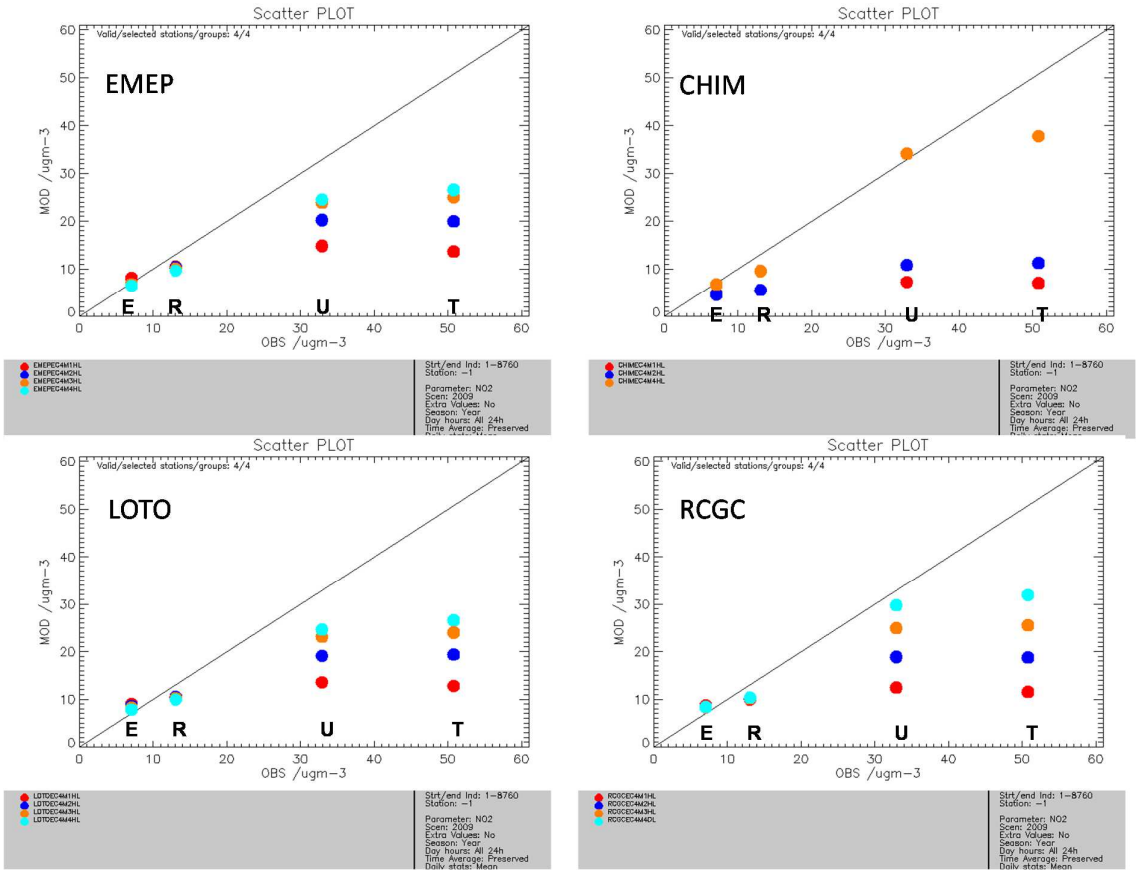

Figure 6. Yearly averaged NO2 concentrations per station type (from left to right: EMEP , Rural, Urban, Traffic) for the 4 spatial resolution (light blue 7 km, orange 14 km, dark blue 28 km, red 56 km). U and T groups are based on a radius of 30 km, E and R on 200km radius.

One of the major causes of these model resolution increments is the emissions, and in particular the differences between emission densities at fine and coarse resolutions. Figure 7 illustrates the relation between concentration deltas (Concentration [7km] – Concentration [56km]) and emission deltas (Emission [7km] – Emission [56km]). As seen from this figure most of the concentration increment (delta) can be explained by the emission delta. The spread around the trend line provides some

information on the importance of other factors such as the local meteorological or the role of chemistry. Most of this additional spread happens in stations belonging to countries like Italy, Greece, Portugal and Spain.

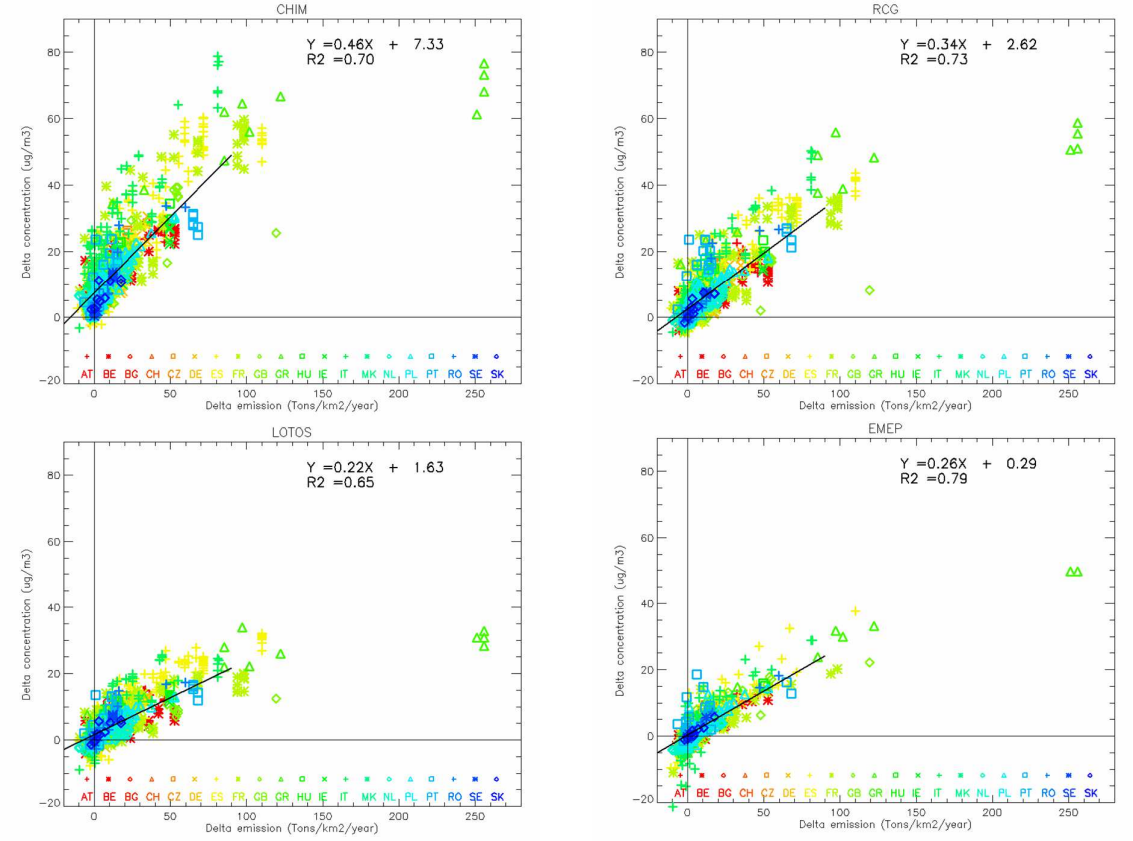

Figure 7. Relation between NO2 concentrations (µg/m3) deltas and NOx emission deltas between 56 and 7 km resolutions. Stations are indicated per country.

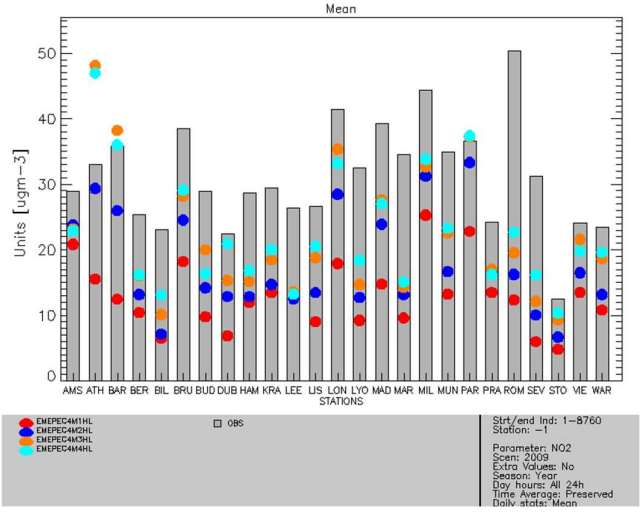

Figure 8. Yearly NO2 averaged grid increments per city areas for urban background stations at the 4 spatial resolutions (red 56 km, dark blue 28 km, orange 14 km, light blue7 km)

In Figure 8 the annual mean NO2 concentrations at the urban stations is given per agglomeration. In this picture the same reduction in the bias is observed as given in Figure 5. Here it can be seen that the response per agglomeration is variable. Difference for Hamburg are very small, whereas the increase as function of resolution is large for London. Comparing the red and light blue dots shows that the pattern across the agglomerations also changes. The spatial variation is further looked at in Figure 9. These show that the explained spatial variability improves as function of resolution. Moreover, the slope of the fits increase significantly indicating that the models explain the magnitude of the variability between urban regions better.

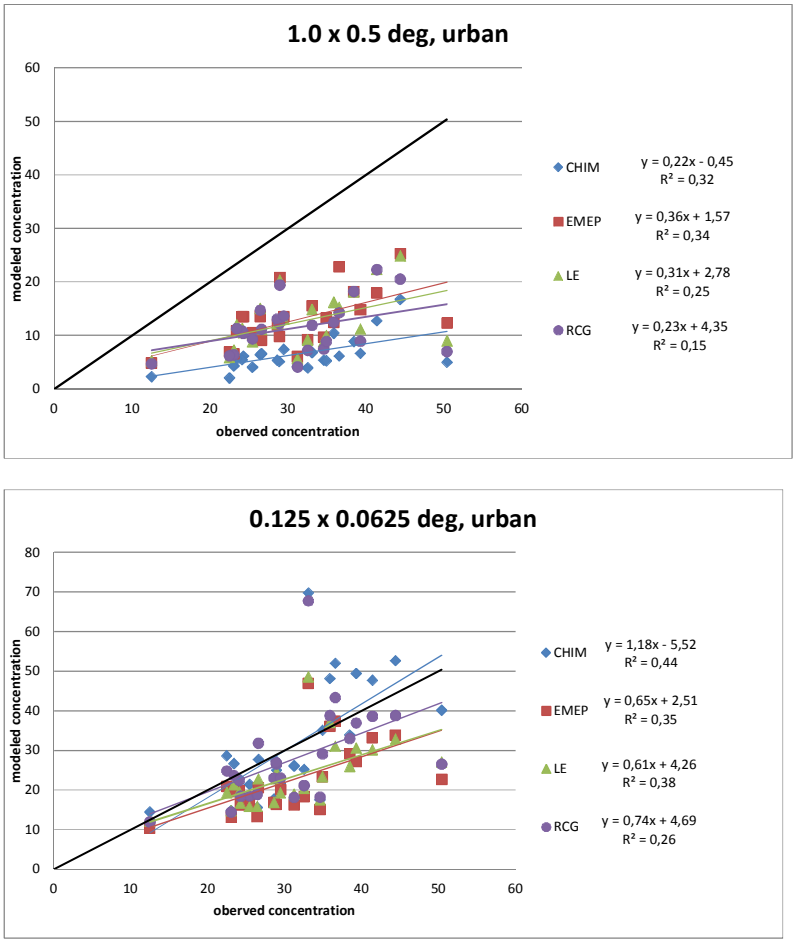

Figure 9. comparison of observed and modelled annual average concentrations of NO2 for the urban agglomerations. For the 56 Km (upper panel) and 7 Km (lower panel) the fits parameters are shown.

A summary of the spatial statistical analysis for NO2 is given in Figure 10. The main findings are:

- Spatial correlation increases with resolution increase. Response is quite variable among models, but largest gain appears to occur between 56 and 28 Km.
- Bias for NO2 is significantly reduced for the urban group, slope of regression line increases significantly.
- 14 and 7 Km resolution have very similar average biases, spatial correlations and slopes

- As expected performance at rural sites stable with resolution, though for the spatial correlation a slight increase in performance may be observed at the cost of a slight increase in bias.

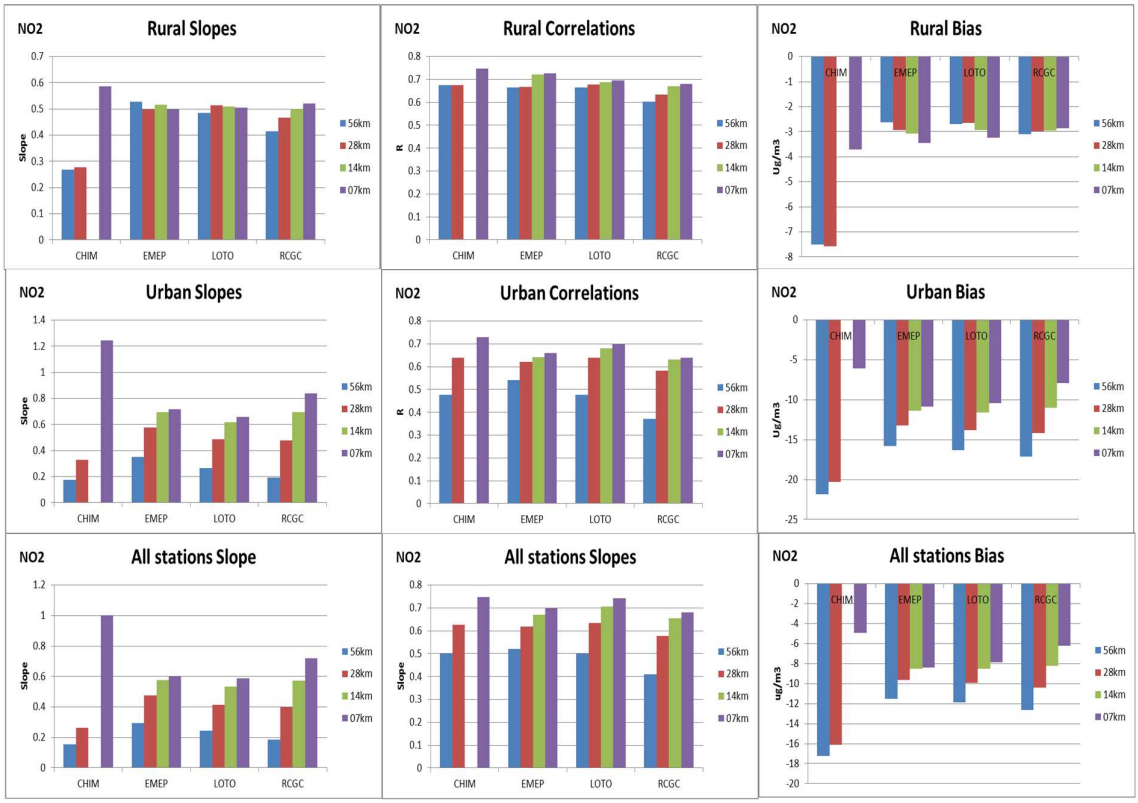

Figure 10. Summary of statistical analysis for NO2. Note the different scales between the station groups

3.3.2 PM10

In Figure 11 the annual average PM10 concentrations are grouped by station types. Also for PM10, the grid resolution increment is very weak at AIRBASE rural and EMEP stations in all models. Models exhibit a similar behavior in terms of impact of resolution but the magnitude is different. Urban increments are similar for the LOTOS-EUROS and RCG, whereas for EMEP they are significantly lower. We explain this by the difference in the surface layer depth, being deeper in EMEP. Note that these three models show more or less the same steps for each increase in resolutions. CHIMERE however shows a large jump in urban concentrations between 14 and 7 Km resolution, even affecting the rural levels, and likely explained by the urban mixing parameterization.

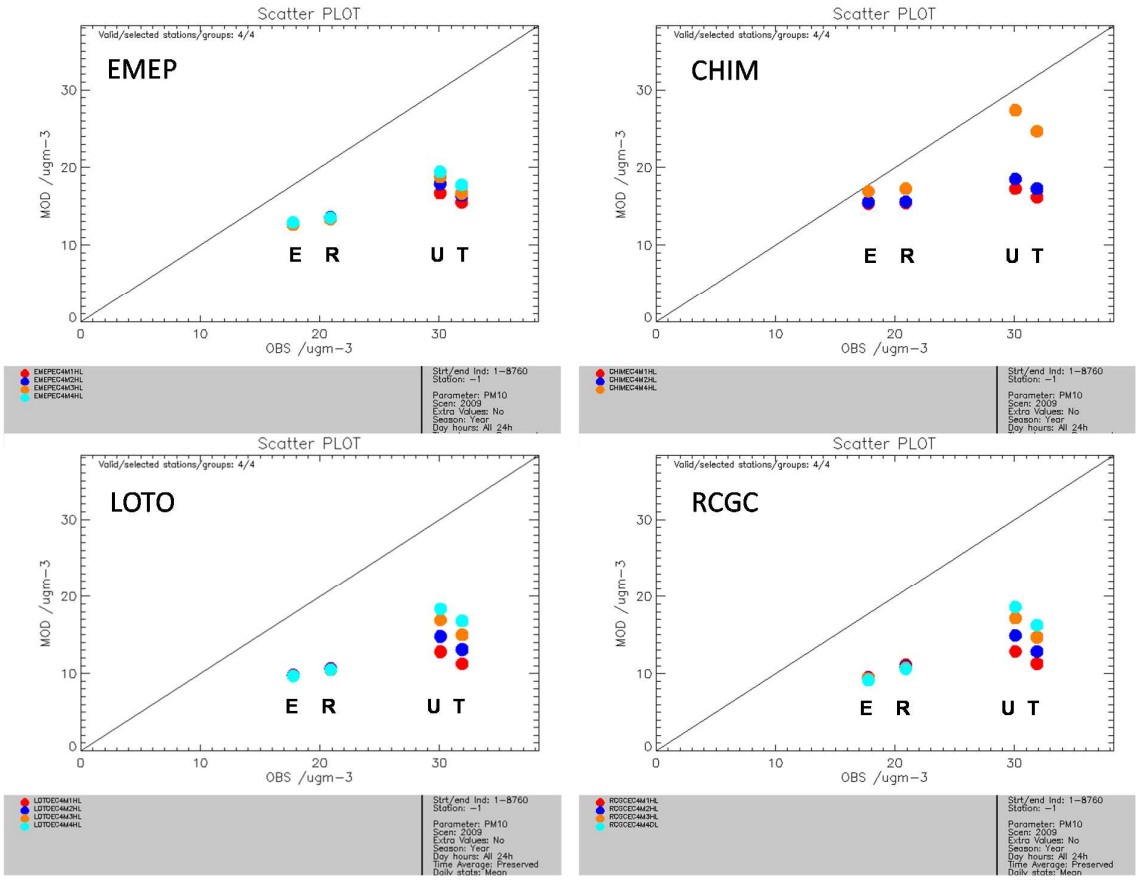

Figure 11. Yearly averaged PM10 concentrations per station type (from left to right: EMEP , Rural, Urban, Traffic) for the 4 spatial resolution (light blue 7 km, orange 14 km, dark blue 28 km, red 56 km). U and T groups are based on the 30 km radius ; E and R groups are based on a radius of 200 km.

A summary of the spatial statistical analysis for PM10 is given in Figure 12. The main findings are:

- Spatial correlation is hardly affected by resolution change but the slope is significantly improved with higher resolution as a result of a lower bias at urban stations.
- Bias for PM10 reduced at urban locations by almost 4 µg/m^3 for RCG and LOTOS-EUROS, whereas the EMEP bias reduces about 2 µg/m^3. CHIMERE shows the largest increase in PM levels in urban areas lowering the bias by 8 µg/m^3 at 7 Km resolution.
- Performance at rural sites stable with resolution in all models.
- Note that the models include different components to PM10, making it hard to draw conclusions on the differences between the models, especially for the bias.
- The additional increase of PM10 concentrations between 14 and 7 Km resolution in CHIMERE in comparison to the other models can be explained by the adopted vertical mixing scheme as function of urban land cover fraction in CHIMERE.

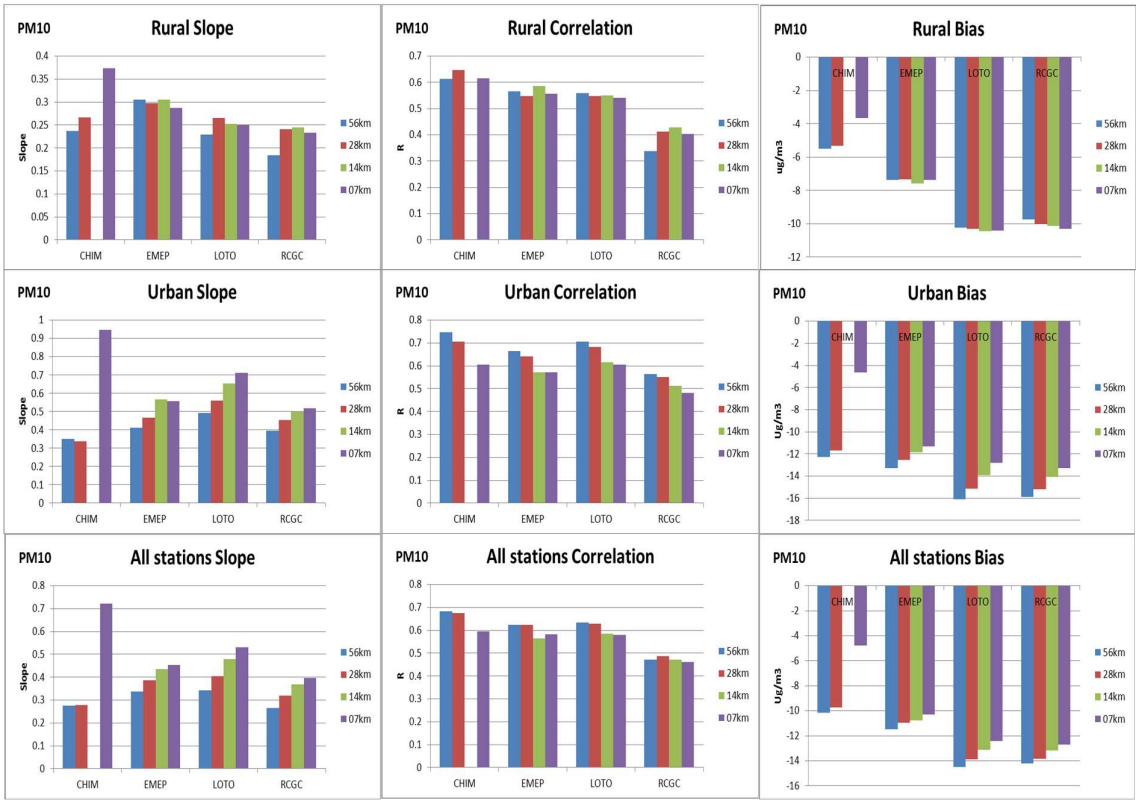

Figure 12. Summary of statistical analysis for PM10. Note the different scales between the station groups

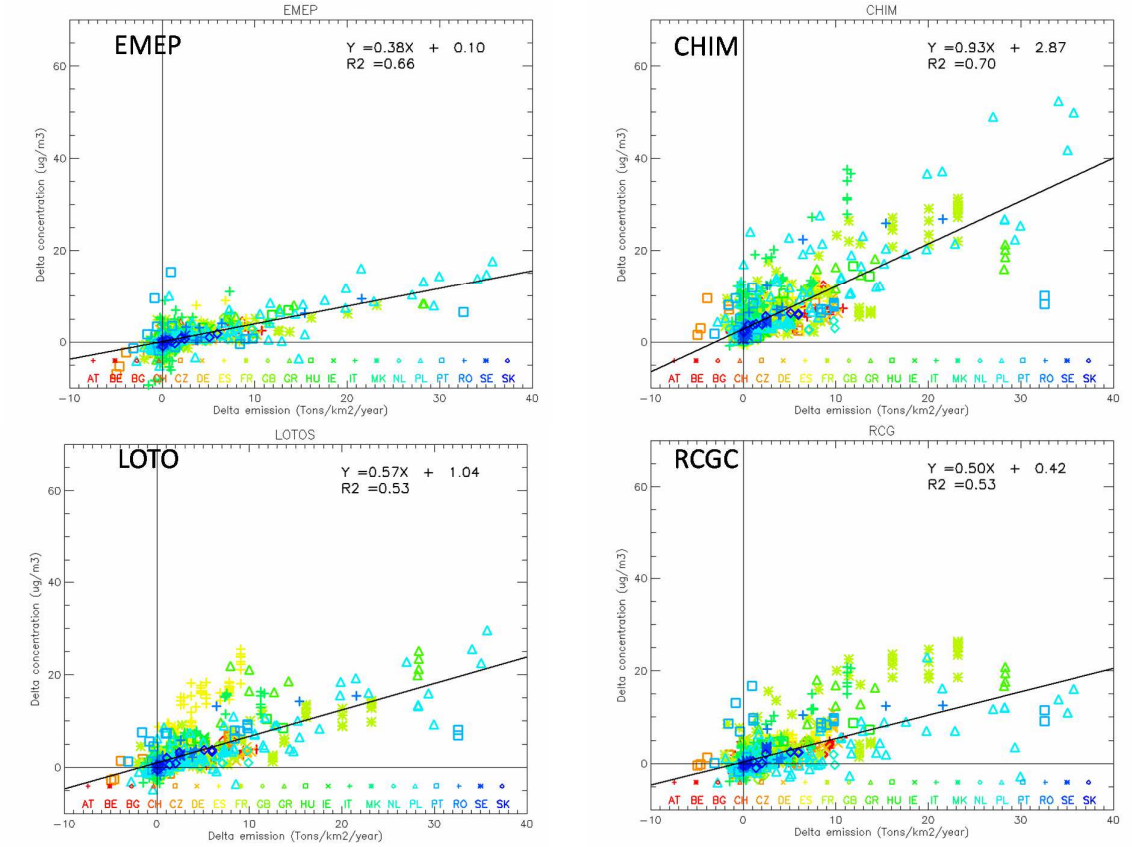

Figure 13. Relation between concentrations (µg/m3) and PPM emission deltas between 56 and 7 km resolutions. Stations are indicated per country.

As for NO2, a significant part (~70%) of the concentration increment (7-56 km) can be explained by the emission density increment as demonstrated by the high values of R^2 (Figure 13). This is mostly seen for EMEP and CHIMERE whereas some additional variance in the concentration increments is seen for the other models. Most of this additional variance happens in stations belonging to countries like Italy, Greece, Portugal and Spain. As expected, CHIM clearly shows the most intense response followed by LOTOS-EUROS and RCG whereas EMEP exhibits significantly lower increments.

The absolute grid effect for PM10 is lower than for NO2, as explained by the higher importance of the rural background levels containing secondary material for PM10. On the other hand, the slopes for PM10 expressing the concentration increase per unit emission are steeper than for NO2. Possible explanation for the steeper slopes and slightly different behavior for PM10 in comparison to NO2 may lie in the fact that NO2 increments may be limited due to the availability of ozone as NO2 is formed through titration of ozone.

3.3.3 Ozone

For ozone we focus our analysis on the model performance for the daily maximum of the running 8 hour mean. The reason is that the analysis is then focussed on the high ozone regime during daytime, and is less sensitive to the impact of differences between models on night time mixing and titration. First, the annual average O3Max8Hr levels (Figure 14) show a different behavior than PM and NO2. Due to the secondary nature of ozone combined with the titration impact of NOx emissions near sources the levels are lower inside a city than outside. The average pattern as function of station type and the response to a resolution change between all models is very similar. Average levels for urban stations decrease towards the observed values for all models.

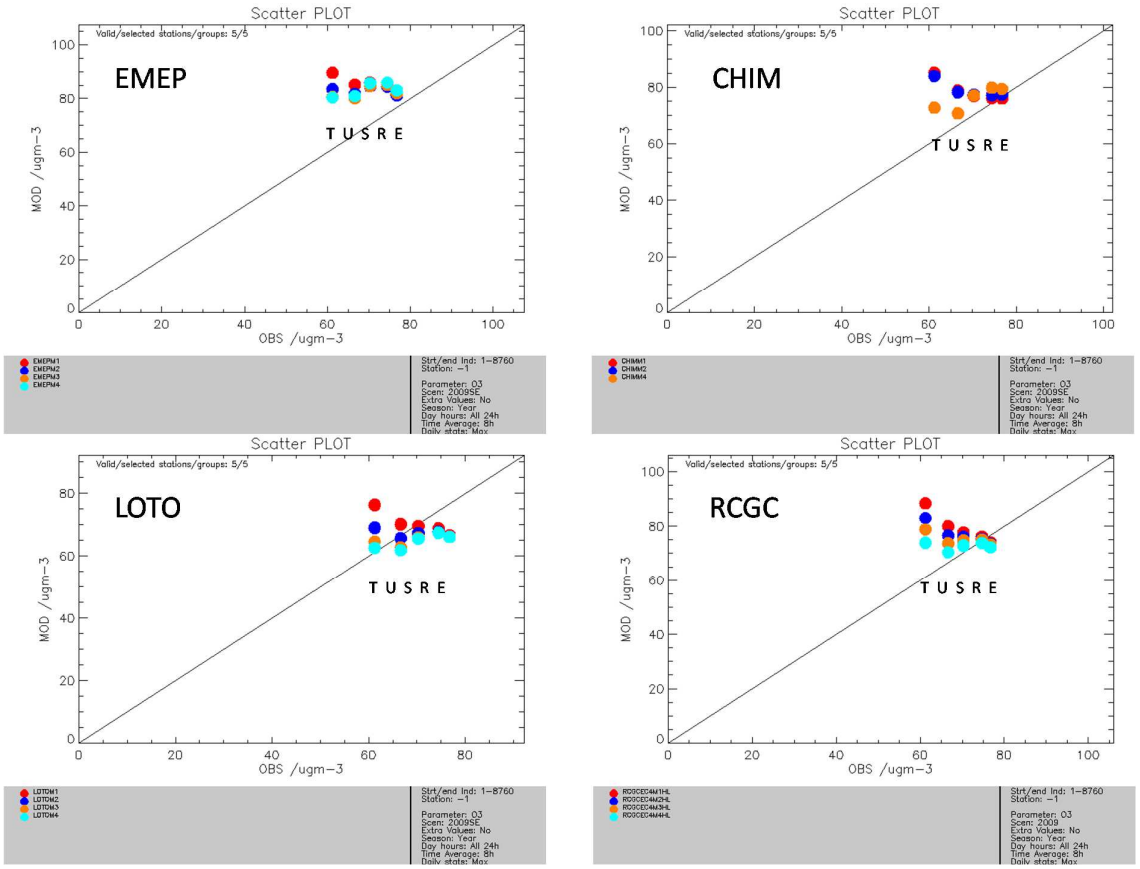

Figure 14. Yearly averaged ozone concentrations per station type (from left to right: EMEP , Rural, SubUrban, Urban, Traffic) for the 4 spatial resolution (light blue 7 km, orange 14 km, dark blue 28 km, red 56 km). U, S and T groups are based on the 30 km radius ; E and R groups are based on a radius of 200 km

The model performance evaluation shows that the models do not respond to the resolution change in the rural areas (Figure 15). Statistical parameters are more or less constant. Increasing resolution has a peculiar effect for the urban locations. The bias shows a minimum at 28 or 14 Km, showing that the increase in model resolution at these resolutions incorporate a better signal of the urban titration effect. Spatial correlation, however, decreases with resolution. In the coarse runs the models capture the gradients in regional background values across Europe quite well (R~0.8). However, increasing resolution and adding more local variability decreases the representation of the spatial contrasts, although for NO2 the spatial patterns become better between cities. This may mean that it is not the variability in NOx emission source strengths between the urban regions is the most important

uncertainty for ozone gradients during the day at these scales. Instead, differences in mixing regimes, chemical regimes and uncertainties in VOC speciation could be more important.

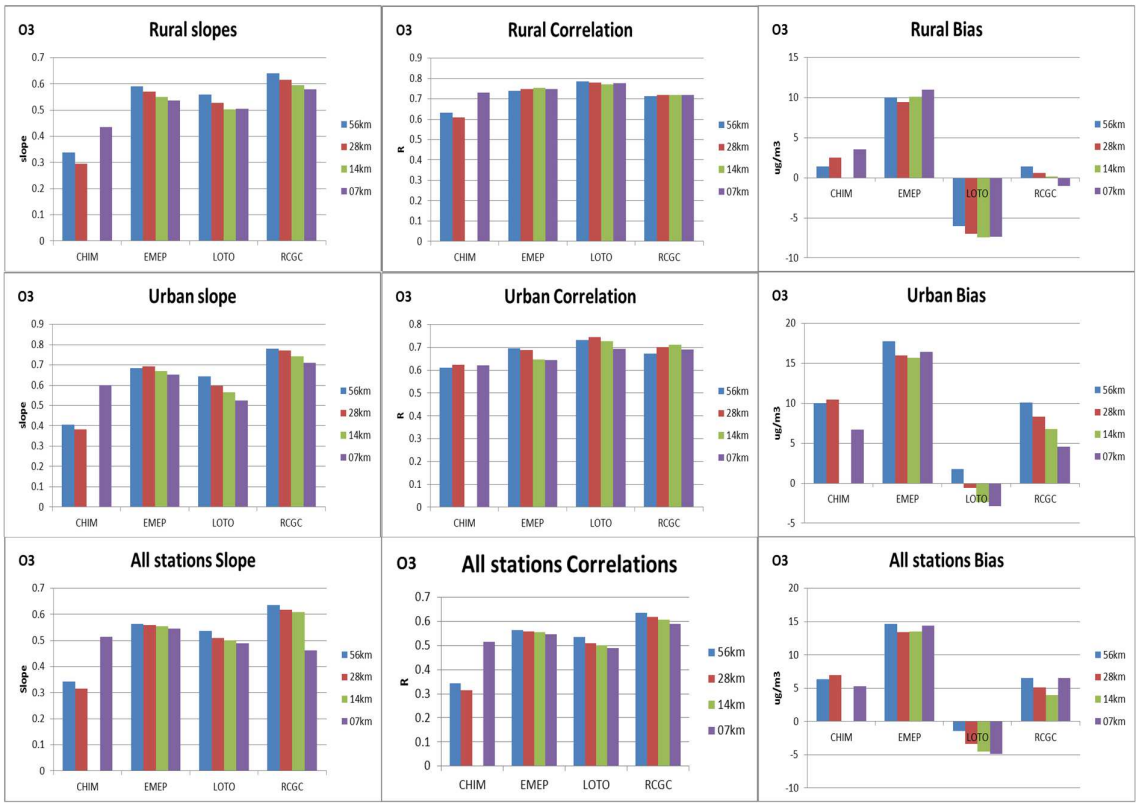

Figure 15. Summary of statistical analysis for O3Max8hr. Note the different scales between the station groups

4. Discussion and conclusions

The exercise showed that the model responses to an increase in resolution show a broadly consistent picture among all models.

It should be noted that the response is more significant for CHIMERE simulations compared to the other participating models. It seems to be due to a specific treatment of the mixing parameterization over urban areas. This point is still investigated by INERIS with sensitivity analyses.

The analysis showed that the grid size does not play a major role for air quality model calculations, which are targeted on the determination of the background (non-urban) air quality. Downscaling model resolution does not change concentration estimations and model performance at rural and EMEP sites.

The grid resolution plays an important role in agglomerations characterized by high emission densities. The urban signal, i.e. the concentration difference between high emission areas and their surroundings, usually increases with decreasing grid size and. This grid effect is more pronounced for NO2 than for PM10, because a large part of the urban PM10 mass consists of secondary components. This part of the PM10 mass is less affected by a decreasing grid size in contrast to the locally emitted primary components.

The grid effect differs between urban regions. The strength of the urban signal is a function of local emissions conditions (extension of the emission areas, emission density, emission gradient, etc.) and meteorological conditions determining ventilation efficiency. For similar emission conditions, regions with weak wind conditions will show a stronger urban signal than well ventilated regions.

For all models, increasing model resolution improves the model performance at stations near large conglomerations as reflected by lower biases for all components and increased spatial correlation for primary components.

As about 70% of the model response to grid resolution is determined by the difference in emission strength, improved knowledge on spatial variation in emission at high resolution is key for the improvement of modeled urban increments. For this purpose one relies on the replacement of currently used top-down European wide data with national expertise.

It is difficult to define a grid size that is adequate to resolve the urban signal under all conditions occurring in a European-wide modeling area. Ideally, a grid size in the range of a few km down to 1 km should be chosen. Such a small grid size is not feasible for regional model applications because the data demands and operating requirements are far too large. If the main emphasis of a model application is targeted on the determination of background air quality for rural areas and large agglomerations, the grid scale M2 (0.5° Longitude and 0.25° Latitude) or, if the data and operational requirements can be fulfilled, the grid scale M3 (0.25° Longitude and 0.125° Latitude) seems to be a good compromise between a pure background application and an application which reproduces most of the urban signals (M4 resolution or even higher).

The limited impact on regional scale model performance shows that a continuing effort is needed to better understand atmospheric processes and interactions with the surface, and to improve our knowledge on emissions (amount, speciation, location and timing).

5. Acknowledgement

The modeling teams that provided input to this exercise were funded through their own channels. The RCG modeling team was funded by Umweltbundesamt Germany, project number 21981. The LOTOS-EUROS modeling team was funded by the Dutch Ministry for Infrastructure and Environment.

6. References

Thunis, E. Georgieva, A. Pederzoli, 2011. The DELTA tool and Benchmarking Report template: Concepts and User's Guide Version 1. P.. Fairmode report, http://fairmode.ew.eea.europa.eu/

Vautard, R., B.Bessagnet, M.Chin, and Menut, L.: On the contribution of natural Aeolian sources to particulate matter concentrations in Europe: testing hypotheses with a modelling approach, Atmospheric Environment, 39, 3291–3303, 2005.

7. Appendices

7.1 EMEP model description

The EMEP MSC-W (Meteorological Synthesizing Centre -West) model is a development of the 3-D chemical transport model of Berge and Jakobsen (1998), extended with photo-oxidant and inorganic aerosol chemistry (Andersson-Sköld and Simpson, 1999; Simpson et al., 2003, 2012), and organic aerosol modules (Bergström et al., 2012). In this exercise we use model version rv4beta12, which is identical to the rv4 version documented in Simpson et al. (2012) except for some minor updates.

The model includes 20 vertical layers, using terrain-following coordinates; the lowest layer has a thickness of about 90m. The meteorological fields for 2009 are derived from the European Centre for Medium Range Weather Forecasting Integrated Forecasting System (ECMWF-IFS) model (http://www.ecmwf.int/research/ifsdocs/).

The model uses essentially two modes for particles, fine and coarse aerosol, although assigned sizes for some coarse aerosol vary with compound. The parameterization of the wet deposition in the model is based on Berge and Jakobsen (1998) and includes in-cloud and sub-cloud scavenging of gases and particles. Further details, including scavenging ratios and collection efficiencies, are given in Simpson et al. (2012).

Boundary concentrations of most long-lived model components are set using simple functions of latitude and month (see Simpson et al., 2012 for details). For ozone more accurate boundary concentrations are needed and these are based on climatological ozone-sonde data-sets, modified monthly against clean air surface observations at Mace Head on the west coast of Ireland (Simpson et al., 2012).

Berge, E. and Jakobsen, H. A.: A regional scale multi-layer model for the calculation of long-term transport and deposition of air pollution in Europe, Tellus, 50, 205–223, 1998.

Andersson-Sköld, Y. and Simpson, D.: Comparison of the chemical schemes of the EMEP MSC-W and the 985 IVL photochemical trajectory models, Atmos. Environ., 33, 1111–1129, 1999.

Simpson, D., Fagerli, H., Jonson, J., Tsyro, S., Wind, P., and Tuovinen, J.-P.: The EMEP Unified Eulerian Model. Model Description, EMEP MSC-W Report 1/2003, The Norwegian Meteorological Institute, Oslo, Norway, 2003.

Simpson, D., Benedictow, A., Berge, H., Bergström, R., Emberson, L. D., Fagerli, H., Flechard, C: Hayman, G. D., Gauss, M., Jonson, J. E., Jenkin, M. E., Nyíri, Á., Richter, C., Semeena, V. S., Tsyro, S., Tuovinen, J.-P., Valdebenito, A., and Wind, P.: The EMEP MSC-W chemical transport model – technical description, Atmos. Chem. Phys. 12, 7825-7865, doi:10.5194/acp-12-7825-2012, http://www.atmos-chem-phys.net/12/7825/2012/, 2012.

Bergström, R., Denier van der Gon, H.A.C.; Prévôt, A.S.H., Yttri, K.E., and Simpson, D.: Modelling of organic aerosols over Europe (2002-2007) using a volatility basis set (VBS) framework: application of different assumptions regrading the formation of secondary organic aerosols. Atmos. Chem. Phys. Discuss, 12, 5425-5485, 2012.

7.2 CHIMERE model description

CHIMERE is designed to calculate the concentrations of usual chemical species that are involved in the physic-chemistry of the low troposphere. CHIMERE has been described in detail several times: Schmidt et al. (2001) for the dynamics and the gas phase module; Bessagnet et al. (2004, 2008, 2009) for the aerosol module. The aerosol model species are sulphates, nitrates, ammonium, secondary organic aerosol (SOA), sea-salt and dust. The particles size distribution ranges from 40 nm to 10 µm and are distributed into 8 bins (0.039, 0.078, 0.156, 0.312, 0.625, 1.25, 2.5, 5, 10 µm). For more detail on the latest development one can refer to the online documentation :

(http://www.lmd.polytechnique.fr/chimere).

A coarse domain encompassing the four nested domain has been defined with **a 50 km resolution**. Boundary conditions are monthly mean climatologies taken from the LMDz-INCA (Schulz et al. 2006) model for gaseous species and from the GOCART model (Ginoux et al., 2001) for aerosols (desert dust, carbonaceous species and sulphate). Within EC4MACS, the vertical resolution has been improved close to the ground level. Nine vertical levels are selected with a **first layer height raising at 20-25 m**.

Six biogenic species (isoprene, α-pinene, β-pinene, limonene, ocimene, and NO) were calculated using the MEGAN model (Guenther et al., 2006). We also accounted for fire emissions from GFED. The fire emissions GFED (Global Fire Emissions Database) are derived from satellite observations (Giglio et al., 2010). These emission data are monthly climatologies available on the 1996-2009 period at 0.5 ° resolution over Europe. Only fire emissions of CO, NOx, SO2 and PM components have been considered in CHIMERE.

Correction of meteorology on urban areas in CHIMERE

In dispersion models at the urban scale, the lower part of the boundary layer is often represented using parameterizations derived from the theory of similarity of the surface layer. The urban effects are then considered by changes in surface roughness and heat flux. Nevertheless, these formulations should only be used in the inertial sublayer (ISL) which is well above the tops of the building.

Indeed, in the sub-rough layer (RSL or urban sublayer), *i.e.* in the immediate vicinity of the urban canopy elements, the flow has a rather complex structure (Raupach, 1980) and the similarity theory cannot be applied. Rotach (1993ab, 1995) analyzed mean flow and turbulence measurements inside and above an urban street canyon. He found that one of the characteristic features of the RSL is an increase in the absolute value of Reynolds stress, from essentially zero at the average zero plane displacement height up to a maximum value, which he observed at about two times the average building height. The RSL extends from the ground to a level where horizontal homogeneity of the flow is well established, so about 2 to 5 times the average height of the elements of the canopy (Raupach et al., 1991) or up to several tens of meters in major cities. In a first approach, the Schmidt number defined by the ratio of diffusivity of momentum and mass diffusion coefficient is taken equal to 1. Considering this, Kz is given by :

$$Kz = \frac{-\overline{u'w'}}{\frac{\partial u}{\partial z}}$$

Considering this, we can assume at urban ground level a negligible value of Kz. Then Kz should increase with the Reynolds stress to a maximum value at 2 to 5 times the average height of the buildings.

This first level of CHIMERE is currently 20 m. This is clearly two times under the average of the buildings height in big cities. So that we can assume that the corresponding Reynolds stress at this level has not yet reach his maximum value and the corresponding value of Kz is overestimate even if we can also assume that Kz is underestimate at the second level of CHIMERE. At the first level of CHIMERE, Kz should be given by :

$$Kz = \int_{z=0}^{z=1st\ level} \frac{-\overline{u'w'}}{\frac{\partial u}{\partial z}}\, dz$$

In a first approach, if we assume that the theory of similarity is applicable above the first level, we can take for urban areas :

$$Kz\ (z < first\ level) = \frac{Kz\ (first\ level\ computed\ with\ the\ similarity\ theroy)}{2}$$

This coefficient is applied to correct the wind speeds in the first CHIMERE layer so as to limit the advection of primary pollutants close to the ground. This coefficient is a compromise between several values reported in the literature.

References :

Bessagnet, B., A. Hodzic, R. Vautard, M. Beekmann, S. Cheinet, C. Honoré, C. Liousse, L. Rouil, Aerosol modeling with CHIMERE—preliminary evaluation at the continental scale, *Atmospheric Environment*, Volume 38, Issue 18, June 2004, Pages 2803-2817, ISSN 1352-2310, 10.1016/j.atmosenv.2004.02.034, **2004**.

Bessagnet B., L.Menut, G.Curci, A.Hodzic, B.Guillaume, C.Liousse, S.Moukhtar, B.Pun, C.Seigneur, M.Schulz Regional modeling of carbonaceous aerosols over Europe - Focus on Secondary Organic Aerosols, *Journal of of Atmospheric Chemistry*, 61, 175-202, **2009**.

Bessagnet B., L.Menut, G.Aymoz, H.Chepfer and R.Vautard, Modelling dust emissions and transport within Europe: the Ukraine March 2007 event, *Journal of Geophysical Research - Atmospheres*, 113, D15202, doi:10.1029/2007JD009541, **2008**.

Giglio, L., Randerson, J. T., van der Werf, G. R., Kasibhatla, P. S., Collatz, G. J., Morton, D. C., and DeFries, R. S.: Assessing variability and long-term trends in burned area by merging multiple satellite fire products, *Biogeosciences*, 7, 1171-1186, doi:10.5194/bg-7-1171-2010, **2010**.

Ginoux, P., Chin, M., Tegen, I., Prospero, J.M., Holben, B., Dubovik, O., Lin, S.-J., Sources and distributions of dust aerosols simulated with the GOCART model. *Journal of Geophysical Research* 106, 20,255–20,273, **2001**.

Guenther, A., Karl, T., Harley, P., Wiedinmyer, C., Palmer, P., Geron, C., 2006. Estimates of global terrestrial isoprene emissions using MEGAN (Model of Emissions of Gases and Aerosols from Nature). Atmos. Chem. Phys. 6, 31813210, **2006**.

Schmidt, H., Derognat, C., Vautard, R., Beekmann, M. A comparison of simulated and observed ozone mixing ratios for the summer of 1998 in western Europe. *Atmospheric Environment* 35, 6277–6297, **2001**.

Schulz, M., Textor, C., Kinne, S., Balkanski, Y., Bauer, S., Berntsen, T., Berglen, T., Boucher, O., Dentener, F., Guibert, S., Isaksen, I.S.A., Iversen, T., Koch, D., Kirkevå g, A., Liu, X., Montanaro, V., Myhre, G., Penner, J.E., Pitari, G., Reddy, S., Seland, O., Stier, P., Takemura, T., Radiative forcing by aerosols as derived from the AeroCom present-day and pre-industrial simulations. *Atmos. Chem. Phys*. 6, 5225–5246, **2006**.

Raupach, M. R., 'A Wind-Tunnel Study of Turbulent Flow Close to Regularly Arrayed Roughness elements, *Boundary-Layer Meteorol*. 18, 373–397, **1980**.

Raupach,M. R.,Antonia R. A., and Rajagopalan S. 'Rough-Wall Turbulent Boundary Layers, *Appl. Mech. Rev*. 44, 1–25, **1991**.

Rotach, M. W.: 'Turbulence Close to a Rough Urban Surface, Part I: Reynolds Stress, *Boundary-Layer Meteorol*. 65, 1–28, **1993a**.

Rotach, M. W.: 'Turbulence Close to a Rough Urban Surface, Part II: Variances and Gradients, *Boundary-Layer Meteorol*. 66, 75–92, **1993b**.

7.3 LOTOS-EUROS model description

In this study we used LOTOS-EUROS v1.8, a 3-D regional CTM that simulates air pollution in the lower troposphere. Previous versions of the model have been used for the assessment of (particulate) air pollution (e.g. Schaap et al., 2004a; 2004b; 2009; Barbu et al., 2009; Manders et al., 2009; 2010). For a detailed description of the model we refer to Schaap et al. (2008), Wichink Kruit et al. (2012) and abovementioned studies. Here, we describe the most relevant model characteristics and the model simulation performed in this study.

The model uses a normal longitude–latitude projection and allows to specify the model resolution and domain within its master domain encompassing Europe and its periphery. The model top is placed at 3.5 km above sea level and consists of three dynamical layers: a mixing layer and two reservoir layers on top. The height of the mixing layer at each time and position is extracted from ECMWF meteorological data used to drive the model. The height of the reservoir layers is set to the difference between ceiling (3.5 km) and mixing layer height. Both layers are equally thick with a minimum of 50 m. If the mixing layer is near or above 3500 m high, the top of the model exceeds 3500 m. A surface layer with a fixed depth of 25 m is included in the model to monitor ground-level concentrations.

Advection in all directions is handled with the monotonic advection scheme developed by Walcek (2000). Gas phase chemistry is described using the TNO CBM-IV scheme (Schaap et al., 2009), which is a condensed version of the original scheme by Whitten et al. (1980). Hydrolysis of N_2O_5 is described following Schaap et al. (2004a). Aerosol chemistry is represented with ISORROPIA2 (Fountoukis and Nenes, 2007). The pH dependent cloud chemistry scheme follows Banzhaf et al. (2011). Formation of course-mode nitrate is included in a dynamical approach (Wichink Kruit et al., 2012). Dry deposition for gases is modeled using the DEPAC3.11 module, which includes canopy compensation points for ammonia deposition (Van Zanten et al., 2010). Deposition of particles is represented following Zhang et al. (2001). Stomatal resistance is described by the parameterization of Emberson et al. (2000a,b) and the aerodynamic resistance is calculated for all land use types separately. Wet deposition of trace gases and aerosols are treated using simple scavenging coefficients for gases (Schaap et al., 2004b) and particles (Simpson et al., 2003). The model set-up used here does not contain secondary organic aerosol formation or a volatility basis set approach as we feel that the understanding of the processes as well as the source characterization are too limited for the current application.

7.4 REM-CALGRID (RCG) model description

Overview

REM-CALGRID is an urban/regional scale chemical Eulerian grid model development. Rather than creating a completely new model, the urban-scale photochemical model CALGRID (Yamartino et al., 1992) and the regional scale model REM3 (Stern, 1994; Hass et al., 1997; Römer et al., 2003) were used as the starting point for the new urban/regional scale model, REM-CALGRID (RCG). The premise was to design an Eulerian grid model of medium complexity that fulfills the requirements of the European Commission's ambient air quality framework directive 96/62/EC (FWD) on air quality modeling. The directive demands that a model must be capable of hourly predictions for periods of a year or more. To comply with these preconditions, RCG can be used on the regional and the urban scale for short-term and long-term simulations of oxidant and aerosol formation.

The model includes the following features:

- A generalized horizontal coordinate system, including latitude-longitude coordinates;
- A vertical transport and diffusion scheme that correctly accounts for atmospheric density variations in space and time, and for all vertical flux components when employing either dynamic or fixed layers;
- A new methodology to eliminate errors from operator-split transport and to ensure correct transport fluxes, mass conservation, and that a constant mixing ratio field remains constant;
- Inclusion of the recently improved and highly-accurate, monotonic advection scheme developed by Walcek (2000). This fast and accurate scheme has been further modified to exhibit even lower numerical diffusion for short wavelength distributions;
- The latest release of the CBM-IV photochemical reaction scheme;
- The ISORROPIA equilibrium aerosol modules, that treats the thermodynamics of inorganic aerosols;
- An simplified version of the SORGAM equilibrium aerosol module, that treats the thermodynamics of organic aerosols;
- Simple modules to treat the emissions of sea salt aerosols and wind-blown dust particles;
- A simple wet scavenging module based on precipitation rates;
- An emissions data interface for long term applications that enables on-the-fly calculations of hourly anthropogenic and biogenic emissions;
- One-way-nesting capabilities.

Horizontal and vertical grid system

Pollutant concentrations in RCG are calculated at the center of each grid cell volume, representing the average concentration over the entire cell. Meteorological fields provided externally by a meteorological driver are internally assigned to a staggered grid arrangement. State variables such as temperature, pressure or water vapor are as the pollutants located at cell center, and represent grid cell average conditions. Wind components and diffusion coefficients are defined at cell interfaces to describe the transfer of mass in and out of each cell face, thus allowing to solve the transport equations in flux form.

The RCG model uses a 3-dimensional system of grid cells. Two types of horizontal grids are possible

- a rectangular grid (e.g., Lambert Conformal or UTM), where grid cells are assumed square and always have the same area,
- a geographical grid, where longitude represents east-west location, latitude represents north-south location.

In the vertical the coordinates are terrain following with the top of the modeling domain a fixed height above the local terrain. There are two choices for the vertical grid system:

- An arbitrary, in space and time fixed grid with layer heights,
- A dynamic grid with an arbitrary amount of layers varying in both space and time according to the horizontal and vertical variations of the mixing height.

In RCG, the 1-dimensional, highly-accurate, monotonic advection scheme developed by Walcek (2000) is used for the horizontal advection of pollutants. This algorithm uses a low-spatial-order accuracy definition of within-cell concentrations, coupled with a "steepening" methodology. It exhibits the following features:

- creation of small numerical diffusion,
- good transport fidelity in terms of phase speed, group velocity, and low shape distortion,
- prohibition of negative concentrations,
- ability to cope with space-time varying vertical level structures,
- mass conservation,
- limitations on the creation of new maximum or minimum concentration values, and,
- complete monotonicity of mixing ratios.

Vertical diffusion parameters are derived using the Monin-Obukhov similarity theory for the description of the structure of the diabatic surface layer (K-theory).

Chemistry

An updated version of the lumped gas phase chemistry scheme CBM-4 (Gery et al., 1989), including Carter's 1-Product Isoprene scheme (Carter, 1996), is used for the simulations. Homogeneous and heterogeneous conversion of NO_2 to HNO_3 is added. In addition to gaseous phase, also simple aqueous phase conversion of SO_2 to H_2SO_4, through oxidation by H_2O_2 and ozone, has been incorporated. Equilibrium concentrations for SO_2, H_2O_2 and ozone are calculated using Henry constants and assuming progressive cloud cover for relative humidity above 80%. Effective rate constants for the aqueous phase reactions $SO_2+H_2O_2$ and SO_2+O_3 have been calculated for an average pH of 5 using acid/base equilibrium and kinetic data from Seinfeld and Pandis (1998).

For numerical solution of the chemistry differential equations system, an Eulerian backward iterative method with a variable time step control is used.

Photolysis rates are derived for each grid cell assuming clear sky conditions as a function of solar zenith angle, altitude and total ozone column. The Tropospheric Ultraviolet-Visible Model (TUV) radiative transfer and photolysis model, developed at the National Center of Atmospheric Research (Madronich and Flocke, 1998) is used to provide the RCG model with a multi-dimensional lookup table of photolytic rates.

Aerosol treatment

A bulk approach is used for the aerosol formation, i.e. aerosol growth is not considered and the major PM constituents are treated as a single model species with a given log-normal size distribution. RCG treates two modes: a fine mode (PM<2.5 µm) and a coarse mode (2.5 µm <PM<10 µm).

The equilibrium between gaseous nitric acid, ammonia and particulate ammonium nitrate and ammonium sulphate and aerosol water is calculated with the ISORROPIA thermodynamic module (Nenes et al., 1999) as a function of temperature and humidity.

Production of secondary organic aerosol (SOA) is treated with a simplified version of the SORGAM module (Schell et al., 2001) which calculates the partitioning of semi-volatile organic compounds produced during VOC oxidation between the gas and the aerosol phase.

Overall, in RCG the following different chemical fractions are considered to contribute to PM10, i.e. particulate matter with a dynamical diameter up to 10 µm:

$$PM10=PM_{coarse}+PM2.5_{prim}+EC+OC_{prim}+SOA+SO_4^{2-}+NO_3^-+NH_4^+ +Na^+ +Cl^-$$

PM_{coarse} = mineral coarse particles, emitted by anthropogenic and natural sources

$PM2.5_{prim}$ = mineral fine particles, emitted by anthropogenic and natural sources

EC = elemental Carbon, fine particles, emitted by anthropogenic sources

OC_{prim} = organic Carbon, fine particles, emitted by anthropogenic sources

SO_4^{2-} = sulphate aerosol, fine particles, formed in the atmosphere

NO_3^- = nitrate aerosol, fine particles, formed in the atmosphere

NH_4^+ = ammonium aerosol, fine particles, formed in the atmosphere

SOA = sum of the secondary organic aerosols, formed in the atmosphere

Na^+ = sea salt sodium, coarse particles, emitted by sea water

Cl^- = sea salt chloride, coarse particles, emitted by sea water

Dry and wet deposition

Dry deposition for gaseous species and particles is calculated using the resistance analogy. Turbulent and laminar resistance are calculated from surface roughness, Monin-Obukhov length, friction velocity, molecular diffusivity. Surface resistance is computed following Erisman and Pul (1994) for different surfaces taking into account species dependent (Henry constant, oxidation power), micro-meteorological, and land-use information. For particles, surface resistance is zero. The atmospheric resistances are large for particles in the accumulation mode (0.1 μm<Ø<1 μm), because neither Brownian motion, nor sedimentation are effective pathways; these resistances are calculated for the different species using the fixed size distributions given above. Wet deposition of gases due to in and below cloud scavenging is parameterised as a function of the species dependent Henry constant and the precipitation rate. Wet deposition of particles is treated in RCG using a simple scavenging coefficient approach with identical coefficients for all particles.

Meteorological Input

RCG requires meteorological data at hourly intervals. They consist of the following three-dimensional fields, which must cover the whole three-dimensional model domain:

- U- and V-wind components, temperature, water vapour, density.

Two-dimensional fields are:

- Monin-Obukov-length, friction velocity, precipitation, cloud cover, mixing layer height, surface temperature, surface wind speed, snow cover.

For standard applications, all this meteorological data is produced employing a diagnostic meteorological analysis system based on an optimum interpolation procedure on isentropic surfaces developed at Freie Universität Berlin. The system utilizes all available observed synoptic surface and upper air data as well as topographical and land use information (Reimer and Scherer, 1992). Other data sources can be used, if available.

Emissions input

RCG model requires annual emissions of VOC, NOx, CO, SO_2, CH_4, NH_3, PM10, and PM2.5, split into point and gridded area sources. Mass-based, source group dependent NMVOC profiles are used to break down the total VOC into the different species classes of the chemical mechanisms. Hourly emissions are derived during the model run using sector-dependent, month, day-of-week and hourly emissions factors. PM10 emissions are split into a PM2.5 and a coarse PM (PM10–PM2.5) part, the PM2.5 part is further split into mineral dust, EC and primary OC. EC fractions in PM2.5 emissions for different SNAP sectors are taken from Builtjes et al. (2003). For primary OC, the following crude method is applied to estimate these emissions in a preliminary way: In the 1996 NEI emission data base (http://www.epa.gov/ttn/chief/), an average OC_{prim}/EC emission ratio for all sectors of about two can be derived for the US. This ratio is then applied to Europe regardless of the SNAP sector, i.e. the OC fractions are set as the double of the EC fractions, except if the sum of the two factors would be larger than unity. In this case (f_{EC}>0.33), f_{OC} is set as: $f_{OC}=1-f_{EC}$.

Biogenic VOC-emissions are derived using the emissions factors for isoprene and OVOC (Other VOCs) as described in Simpson et al. (1999). Terpene emission factors are taken from the CORINAIR emission hand-book. The biogenic calculations of trees are based on the land-use data for 115 forest trees (Koeble and Seufert, 2002). Light intensity and temperature dependencies are also

considered. Soil NO emissions are calculated as a function of fertilizer input and temperature following Simpson et al. (1999).

Resuspension of mineral aerosol from natural soils is included as a function of friction velocity and the nature of soil; both the direct entrainment of small particles (Loosemore and Hunt, 2000) and saltation, i.e. the indirect entrainment due to large particles which fall back to the soil and entrain smaller particles (Claiborn et al., 1998) is taken into account.

The sea-salt aerosol emissions (Na+, Cl−) are parameterised according to Gong et al. (1997) and Monahan et al. (1986) as a function of size and wind speed.

Literature

Beekmann M., A. Kerschbaumer, R. Stern, E. Reimer, D. Möller., 2007, PM measurement campaign HOVERT in the Greater Berlin area: model evaluation with chemically specified particulate matter observations for a one year period, Atmos. Chem. Phys.,7, 55-68, 2007

Builtjes, P. J. H.,2003, Aerosols over Europe, Focus on Black carbon, TNO report R2003/146, February 2003.

Carter, W.,1996, Condensed atmospheric photooxidation mechanisms for isoprene, Atmos. Environ., 30, 4275–4290, 1996.

Claiborn, C., Lamb, B., Miller, A., Beseda, J., Clode, B., Vaughan, J., Kang, L., and Nevine, C., 1996, Regional measurements and modeling of windblown agricultural dust: The Columbia Plateau PM10 Program, J. Geophys. Res., 103(D16), 19 753–19 767, 1998.

Erisman, J. and Van Pul, A.,1994, Parameterization of surface resistance for the quantification of atmospheric deposition of acidifying pollutants and ozone, Atmos. Environ., 28, 2595–2607, 1994.

Gery, M. W., Witten, G. Z., Killus, J. P., Dodges, M. C.,1989, A photochemical kinetics mechanism for urban scale and regional scale computering modeling, J. Geophys. Res., 94(D10), 12925–12956, 1989.

Gong, S. L., Barrie, L. A., and Blanchet, J.-P., 1997, Modelling sea-salt aerosols in the atmosphere. 1. Model development, J. Geophys. Res., 102, 3805–3818, 1997.

Hass, H., Bultjes, P. J. H., Simpson, D., and Stern, R.,1997, Comparison of model results obtained with several European regional air quality models, Atmos. Environ., 31, 3259–3279, 1997,

Koeble, R. and Seufert, G., 2002, Novel maps for forest trees in Europe. Proceedings of the 8th European Symposium on the Physico-Chemical Behaviour of Atmospheric Pollutants. JRC Ispra.

Loosemore, G. A. and Hunt, J. R., 2000, Dust resuspension without saltation, J. Geophys. Res., 105(D16), 20 663–20 5 671, 2000.

Madronich, S. and S. Flocke (1998). The role of solar radiation in atmospheric chemistry, in Handbook of Environmental Chemistry (P. Boule, ed.), Springer_Verlag, Heidelberg, pp. 1-26, 1998.

Monahan, E.C, Speil, D., Speil, K. (1986), Oceanic whitecaps. Reidel 1986

Nenes, A., Pilinis, C., and Pandis, S. N.,1999, Continued development and testing of a new thermodynamic aerosol module for urban and regional air quality models, Atmos. Environ., 33, 1553–1560, 1999.

Odum, J. R., Hoffmann, T., Bowman, F., Collins, D., Flagan, R. C., and Seinfeld, J. H.,1996, Gas/Particle partitioning and secondary organic aerosol yields, Environ. Sci. Technol., 30, 2580–2585, 1996.

Reimer, E. und Scherer, B. (1992), An operational meteorological diagnostic system for regional air pollution analysis and long term modeling, in Air Pollution Modelling and its Application IX, eds. H. v. Dop und G. Kallos, NATO Challenges of Modern Society, Kluwer Academic/Plenum Publisher, New York.

Römer, M., Beekmann, M., Bergström, R., Boersen, G., Feldmann, H., Flatøy, F., Honore, C., Langner, J., Jonson, J. E., Matthijsen, J., Memmesheimer, M., Simpson, D., Smeets, P., Solberg, S., Stern, R., Stevenson, D., Zandveld, P., and Zlatev, Z.,2003, Ozone trends according to ten dispersion models, EUROTRAC-2 special report, GSF, Munich, Germany, 2003.

Schell, B., Ackermann, I. J., Hass, H., Binkowski, F., and Ebel, A.,2001, Modelling the formation of secondary organic aerosol within a comprehensive air quality model system, J. Geophys. Res., 106(D22), 28 275–75–28 293, 2001.

Seinfeld, J. and Pandis, S. N.: Atmospheric Chemistry and Physics, John Wiley and Sons, 1998.

Simpson, D., Winiwarter, W., Börjesson, G., Cinderby, S., Ferreiro, A., Guenther, A., Hewitt, C. N., Janson, R., Khalil, M. A. K., Owen, S., Pierce, T. E., Puxbaum, H., Shearer, M., Skiba, U., Steinbrecher, R., Tarrason, L., and Oiquist, M. G.,1999: Inventorying emissions from nature in Europe, J. Geophys. Res., 104(D7), 8113–8152, 1999.

Stern, R., 2003, Entwicklung und Anwendung des chemischen Transportmodells REM-CALGRID. Abschlussbericht zum FuE-Vorhaben 298 41 252 des Umweltbundesamts „Modellierung und Prüfung von Strategien zur Verminderung der Belastung durch Ozon“.

Stern, R., Yamartino, R., Graff, A. (2006). Analyzing the response of a chemical transport model to emissions reductions utilizing various grid resolutions. 28th ITM on Air Pollution Modelling and its Application. May 15-19, 2006, Leipzig, Germany

Stern, R., Builtjes, P., Schaap, M., Timmermans, R., Vautard, R., Hodzic, A., Memmesheimer, M., Feldmann, H., Renner, E., Wolke, R., Kerschbaumer, A. (2008). A model inter-comparison study focussing on episodes with elevated PM10 concentrations. Atmospheric Environment 42 4567-4588. 2008.

Thunis, P., L. Rouil, C. Cuvelier, R.Stern, A. Kerschbaumer, B. Bessagnet, M. Schaap, P. Builtjes, L. Tarrason, J. Douros, N. Moussiopoulos, G. Pirovano, M. Bedogni (2007). Analysis of model responses to emission-reduction scenarios within the CityDelta project, Atmospheric Environment 41 (2007) 208-220

Thunis, P., C. P. Roberts, L. White, L. Post, L. Tarrasón, S. Tsyro, R. Stern, A. Kerschbaumer, L. Rouïl, B. Bessagnet, R. Bergström, M. Schaap, G.A.C. Boersen, P.J.H. Builtjes (2008). Evaluation of a Sectoral Approach to Integrated Assessment Modelling including the Mediterranean

Sea. European Commission Joint Research Centre. Institute for Environment and Sustainability. EUR 23444 EN – 2008.

Van Loon, M., Roemer, M. G. M., Builtjes, P. J. H., Bessagnet, B., Rouil, L., Christensen, J., Brandt, J., Fagerli, H., Tarrason, L., Rodgers, I., Teasdale, I., Stern, R., Bergström, R., Langner, J., and Foltescu, V., 2004, Model intercomparison in the framework of the review of the Unified EMEP model. TNO-report R2004/282, 53 pp. Available at http://www.mep.tno.nl., 2004

Van Loon, L., Vautard,R., Schaap, M., Bergström, R., Bessagnet, B., Brandt, J., Builtjes, P., Christensen, J., Cuvelier, K., Jonson, J., Langner, J., Roberts, L., Rouil, L., Stern, R., Tarrasón, L. Thunis, P., Vignati, P., White, L.,Wind, P. (2007). Evaluation of long-term ozone simulations from seven regional air quality models and their ensemble average. Atmospheric Environment 41, 2083-2097

Vautard, R., Builtjes, P. H. J., Thunis, P., Cuvelier, K., Bedogni, M. Bessagnet, B., Honoré, C., Moussiopoulos, N., Pirovano, G., Schaap, M. Stern, R. Tarrason, L., Wind, P., 2007, Evaluation and intercomparison of Ozone and PM10 simulations by several chemistry-transport models over 4 european cities within the City-Delta project. Atmospheric Environment 41 (2007) 173-188

Walcek, C. J., 2000, Minor flux adjustment near mixing ratio extremes for simplified yet highly accurate monotonic calculation of tracer advection, J. Geophys. Res., 105(D7), 9335–9348, 2000.

Yamartino, R.J., J. Scire, G.R. Carmichael, and Y.S. Chang (1992). The CALGRID mesoscale photochemical grid model-I. Model formulation, Atmos. Environ., 26A (1992), 1493-1512.

Yamartino, R.J., 2003, Refined 3-d Transport and Horizontal Diffusion for the REM/CALGRID Air Quality Model. Bericht zum Forschungs- und Entwicklungsvorhaben 298 41 252 auf dem Gebiet des Umweltschutzes „Modellierung und Prüfung von Strategien zur Verminderung der Belastung durch Ozon“. Freie Universiträt Berlin. Institut für Meteorologie.

Yamartino, R, Flemming, J. Stern, R., 2004, ADAPTATION OF ANA LYTIC DIFFUSIVITY FORMULATIONS TO EULERIAN GRID MODEL LAYERS OF FINITE THICKNESS. ***27th ITM on Air Pollution Modelling and its Application.*** October 25-29***, 2004, Banff, Canada.***

7.5 CMAQv5.0 model description

CALIOPE is an air quality modeling system developed at the Barcelona Supercomputing Center which currently forecasts air quality for Europe and Spain (Baldasano et al. 2011). The system integrates a meteorological model (WRF-ARW), an emission model (HERMES), a chemical transport model (CMAQ) and a mineral dust model (BSC-DREAM8b).

CMAQ has been developed under the leadership of the Atmospheric Modeling Division of the Environmental Protection Agency (EPA) National Exposure Research Laboratory in Research Triangle Park, North Carolina USA. The modeling system and its source codes are freely available for use by air quality regulators, policy makers, industry, and scientists to address multiscale, multi-pollutant air quality concerns. It includes a chemistry transport model that currently allows for the simulation of concentrations and deposition of the major air pollutants. Because of its generalized coordinate system and its advanced nesting features CMAQ can be used to study the behaviour of air pollutant form local to regional scales. A detailed description of the model system is given by Byun and Schere (2006).

There are several comprehensive evaluations of CMAQ which establish model credibility for a wide range of application in USA (e.g. Mebust et al., 2003; Eder and Yu, 2006; Appel et al., 2007, 2008; Simon et al, 2012) and Europe (e.g. Matthias, 2008; Pay et al., 2010; Basart et al., 2012).

The last version of CMAQ modelling system (version 5.0) used in this exercise integrates the last scientific upgrades. The gas-phase oxidations in the atmosphere are described in the CB-05 chemical mechanism (Yarwood et al., 2005).

Aerosols are represented by the modal aerosol module AERO5. Three log-normal modes spanning three size categories Aitken, accumulation and coarse. CMAQv5.0 allows semi-volatile aerosol components to condense and evaporate from the coarse mode and non-volatile sulphate to condense on the coarse mode. Dynamic mass transfer is simulated for the coarse mode, whereas the fine modes are equilibrated instantaneously with the gas phase. CMAQv5.0 simulates oxidative aging reaction for primary organic aerosol as a second order reaction between reduced primary organic carbon and OH radicals (Simon and Bhave, 2012). Additional biogenic precursors such as isoprene and sesquiterpenes were incorporated in version 4.7. New secondary organic aerosol treatment, explained in Carlton et al. (2010), allows three biogenic and four anthropogenic VOC classes to form a variety of semivolatile and nonvolatile products after reacting with gas-phase oxidants. In addition, non-volatile SOA can be formed via aqueous-phase oxidation of glyoxal and methylglyoxal or oligomerization of semivolatile SOA. In total, 19 separate SOA types are formed and tracked. The production of sea salt emission is implemented as a function of wind speed and relative humidity (Gong, 2003; Zhang et al., 2005) form open ocean and surf zone (Clarke et al., 2006). Thermodynamic equilibrium between gas and inorganic fine aerosols is determined by the ISORROPIAv2, is included in CMAQ5.0.

Meteorological input data for the CMAQ model are processed using the WRF-ARW model version v3.3.1.

Concerning natural emissions, MEGAN v2.0 is used to simulate biogenic emission. Furthermore, the long-range transport of mineral dust from Sahara desert is modelled by BSC-DREAM8b.

The CMAQ horizontal grid resolution corresponds to that of WRF-ARW. Its vertical structures was obtained by a collapse from the 38 WRF layers to a total of 15 layers steadily increasing form the surface up to 50 hPa with a stronger density within the PBL. The mean altitude of the lowest layer of CMAQ in CALIOPE system is of 19.5 ± 0.5 m above ground level.

References

Appel, K. W., Bhave, P. V., Gilliland, A. B., Sarwar, G., and Roselle, S. J.: Evaluation of the Community Multiscale Air Quality (CMAQ) model version 4.5: Sensitivities impacting model performance; Part II – particulate matter, Atmos. Environ., 42, 6057–6066, 2008.

Appel, K. W., Gilliand, A. B., Sarwar, G., and Gilliam, R. C.: Evaluation of the Community Multiscale Air Quality (CMAQ) model version 4.5: Sensitivities impacting model performance, Atmos. Environ., 41, 9603–9615, 2007.

Baldasano JM, Pay MT, Jorba O, Gassó S, Jiménez-Guerrero P, 2011. An annual assessment of air quality with the CALIOPE modeling system over Spain. Sci Total Environ, 409, 2163-2178. doi:10.1016/j.scitotenv.2011.01.041.

Basart S, Pay MT, Jorba O, Pérez C, Jiménez-Guerrero P, Schulz M, Baldasano JM, 2012. Aerosol in the CALIOPE air quality modelling system: validation and analysis of PM levels, optical depths and chemical composition over Europe. Atmos Chem Phys, 12, 3363-3392. doi: 10.5194/acp-12-3363-2012.

Byun, D. and Schere, K. L.: Review of the Governing Equations, Computational Algorithms, and Other Components of the Models-3 Community Multiscale Air Quality (CMAQ) Modeling System, Appl. Mech. Rev., 59, 51–77, 2006.

Clarke, A.D., S.R. Owens, and J. Zhou, 2006. An ultrafine sea-salt flux from breaking waves: Implications for cloud condensation nuclei in the remote marine atmosphere. J. Geophys. Res. 111 (D06202).

Eder, B. and Yu, S.: A performance evaluation of the 2004 release of Models-3 CMAQ, Atmos. Environ., 40, 4811–4824, 2006.

Gong, S.L., 2003. A parameterization of sea-salt aerosol source function for sub- and super-micron particles. J. Geophys. Res. 17, 1097. doi:10.1029/2003GB002079.

Matthias, V., 2008. The aerosol distribution in Europe derived with the community multiscale air quality (CMAQ) model: comparison to near surface in situ and sunphotometer measurements. Atmos. Chem. Phys. 8, 5077-5097

Mebust, M. R., Eder, B. K., Binkowski, F. S., and Roselle, S. J.: Models-3 Community Multiscale Air Quality (CMAQ) model aerosol component, J. Geophys. Res., 108(D6), 4184, doi:10.1029/2001JD001410, 2003.

Pay, M.T., Piot, M., Jorba, O., Gassó, S., Gonçalves, M., Basart, S., Dabdub, D., Jiménez-Guerrero, P., Baldasano, J.M., 2010a. A full year evaluation of the CALIOPE-EU air quality modeling system over Europe for 2004. Atmos. Environ. 44, 3322-3342.

Simon H., K. R. Baker and S. Phillips, 2012. Compilation and interpretation of photochemical model performance statistics published between 2006 and 2012. Atmos. Environ. 61, 124-139.

Yarwood, G., Rao, S., Yocke, M., and Whitten, G.: Updates to the Carbon Bond chemical mechanism: CB05. Final report to the US EPA, RT-0400675, available at http://www.camx.com/publ/pdfs/CB05 Final Report 120805.pdf, 2005.

Zhang, Y., Liu, P., Pun, B., Seigneur, C., 2006. A comprehensive performance evaluation of MM5-CMAQ for the summer 1999 southern oxidants study episode, part iii: diagnostic and mechanistic evaluations. Atmos. Environ. 40, 4856-4873. doi:10.1016/j.atmosenv.2005.12.046.